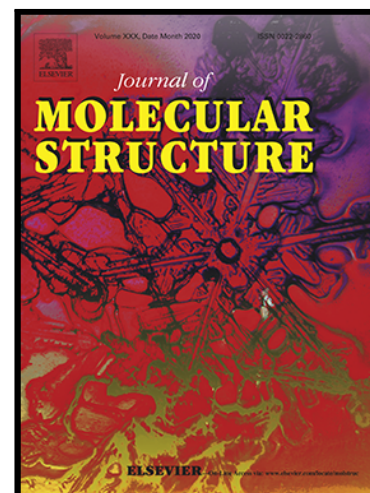


Journal Pre-proof

Design, 3D-QSAR, molecular docking, MD simulations, ADME/Tox properties and DFT study of benzimidazole derivatives as promising α -glucosidase inhibitors



Ayoub Khaldan , Soukaina Bouamrane , Mohamed Ouabane ,
Reda El-mernissi , Marwa Alaqarbeh , Radwan Alnajjare ,
Eda Sönmez Gürer , Savas Kaya , Hamid Maghat ,
Mohammed Bouachrine , Tahar Lakhlifi , Abdelouahid Sbai

PII: S0022-2860(25)00040-7
DOI: <https://doi.org/10.1016/j.molstruc.2025.141351>
Reference: MOLSTR 141351

To appear in: *Journal of Molecular Structure*

Received date: 6 October 2024
Revised date: 30 December 2024
Accepted date: 5 January 2025

Please cite this article as: Ayoub Khaldan , Soukaina Bouamrane , Mohamed Ouabane , Reda El-mernissi , Marwa Alaqarbeh , Radwan Alnajjare , Eda Sönmez Gürer , Savas Kaya , Hamid Maghat , Mohammed Bouachrine , Tahar Lakhlifi , Abdelouahid Sbai , Design, 3D-QSAR, molecular docking, MD simulations, ADME/Tox properties and DFT study of benzimidazole derivatives as promising α -glucosidase inhibitors, *Journal of Molecular Structure* (2025), doi: <https://doi.org/10.1016/j.molstruc.2025.141351>

This is a PDF file of an article that has undergone enhancements after acceptance, such as the addition of a cover page and metadata, and formatting for readability, but it is not yet the definitive version of record. This version will undergo additional copyediting, typesetting and review before it is published in its final form, but we are providing this version to give early visibility of the article. Please note that, during the production process, errors may be discovered which could affect the content, and all legal disclaimers that apply to the journal pertain.

© 2025 Published by Elsevier B.V.

Highlights

- CoMFA and CoMSIA were performed to study 3D-QSAR of the benzimidazole-based oxadiazole derivatives.
- Potent α -glucosidase inhibitors were designed based on the CoMFA and CoMSIA contour maps and assessed *in silico* ADMET.
- A Molecular docking study was carried out to study the interaction between benzimidazole-based oxadiazole ligands and α -glucosidase receptor.
- The stability of protein-ligand interactions between benzimidazole-based oxadiazole derivatives and 3a4a protein was assessed using molecular dynamics (MD) simulations.
- The reactivity and stability of the compounds were discussed in the light of the popular electronic structure principles.

Journal Pre-proof

Design, 3D-QSAR, molecular docking, MD simulations, ADME/Tox properties and DFT study of benzimidazole derivatives as promising α -glucosidase inhibitors

Ayoub Khaldan^{1*}, Soukaina Bouamrane¹, Mohamed Ouabane^{1,2}, Reda El-mernissi¹, Marwa Alaqrbeh³, Radwan Alnajjare^{4,5}, Eda Sönmez Gürer⁶, Savas Kaya^{6*}, Hamid Maghat¹, Mohammed Bouachrine^{1,7}, Tahar Lakhlifi¹ and Abdelouahid Sbai¹

¹Molecular Chemistry and Natural Substances Laboratory, Faculty of Science, Moulay Ismail University, Meknes, Morocco

²Chemistry-Biology Applied to the Environment URL CNRT 13, department of chemistry, Faculty of Science, Moulay Ismail University, Meknes, Morocco

³Department of Chemistry, Faculty of Science, Applied Science Private University, Amman, 11931, Jordan

⁴PharmD, Faculty of Pharmacy, Libyan International Medical University, Benghazi, Libya

⁵Department of Chemistry, Faculty of Science, University of Benghazi, Benghazi, Libya

⁶Sivas Cumhuriyet University, Faculty of Pharmacy, Department of Pharmacognosy, 58140, Sivas/Turkey

⁷EST Khenifra, Sultan Moulay Sliman University, Benimellal, Morocco

E-mail: savaskaya@cumhuriyet.edu.tr

Abstract

Acarbose and miglitol are two distinct α -glucosidase inhibitors that are frequently used to manage diabetes mellitus. Unfortunately, the clinical usage of these medications comes with a number of undesirable side effects. Therefore, development of safer and potent α -glucosidase inhibitor became more necessary. For this reason, a set of 20 benzimidazole-based oxadiazole molecules was addressed using the three-Dimensional Quantitative Structure-Activity Relationship (3D-QSAR) approach. Comparative Molecular Field Analysis (CoMFA) and Comparative Molecular Similarity Indices Analysis (CoMSIA) using steric (S), electrostatic (E) and hydrogen bond donor (D) models showed good statistical outcomes as Q^2 (0.600 and 0.616 respectively) and R^2 (0.958 and 0.928 respectively). The developed models were then validated for their external ability; the R^2 test values were 0.85 and 0.627, respectively. The CoMFA and CoMSIA/SED contour maps helped identify key regions influencing α -glucosidase inhibitory activity, leading to the design of four new benzimidazole-based oxadiazole inhibitors with strong predicted activity. The new recommended compounds confirmed promising consequences in the preliminary *in silico* ADME/Tox prediction. Molecular docking results showed good interactions of compounds M1 and M2 in the active site of the α -glucosidase receptor, and their stability was studied using molecular dynamics simulations throughout 200 ns. The reactivity and stability of compounds M1 and M2 were assessed using the DFT approach, suggesting that these compounds have strong inhibitory potential and may serve as effective anti-diabetic agents, warranting further experimental investigation.

Keywords: 3D-QSAR, Molecular docking, α -glucosidase, benzimidazole, ADME/Tox, DFT.

Introduction

Diabetes mellitus (DM) is a serious health concern that impacts individuals worldwide. It is caused by a lack of insulin secretion and is described by hyperglycemia [1-3]. Complications frequently associated with diabetes mellitus encompass macrovascular issues like coronary heart disease, stroke, and peripheral arterial disease, along with microvascular problems such as diabetic kidney disease, retinopathy, and peripheral neuropathy [4]. The number of cases related to DM increases year by year [5]. According to the International Diabetes Federation, the number of people with diabetes exceeded 366 million in 2011 and is projected to rise significantly to reach 552 million by the year 2030 [6,7]. Lifestyle is a syndrome directly linked with diabetes mellitus, which may cause numerous problems like neuropathy, nephropathy, retinopathy and cardiovascular diseases [8]. Type-2 diabetes mellitus is considered one of the most common types of diabetes in developed countries and is characterized by decreased insulin sensitivity and reduced insulin secretion [9-12]. One of the most effective strategies for managing type-2 diabetes is controlling blood glucose levels by inhibiting the conversion of polysaccharides and oligosaccharides into glucose [13-15]. Treatment using α -glucosidase is an effective method to control type 2 diabetes mellitus as well as other diabetic problems [16-18]. α -Glucosidase is recognized as a crucial enzyme that plays a significant role in the mechanism of DM [19]. α -Glucosidase is an enzyme found in the epithelial lining of the small intestine, and is responsible for catalyzing the final step in the hydrolysis of polysaccharides and disaccharides into glucose [20]. In addition, inhibition of α -glucosidase is important because of the potential effects of reducing postprandial blood glucose, as α -glucosidase activity is related to blood glucose concentrations [21,22]. Miglitol, acarbose and voglibose are α -glucosidase inhibitors clinically adopted in regulatory of the rapid increase of blood glucose [21,23]. However, despite their benefits, these drugs are associated with several adverse effects, such as abdominal pain, diarrhea, and other gastrointestinal issues during long-term treatment [24-26]. Consequently, there is an urgent necessity for new α -glucosidase drugs for the proficient management of DM.

Benzimidazole is an aromatic heterocyclic with an imidazole fused to benzene (Fig.1 (a)). Due to the presence of two nitrogen atoms, this system can function as an acid or a base by donating or receiving protons forming intermolecular interactions [22]. Its properties favor its binding to biological targets; consequently, it has been viewed as a prospective pharmacophore [27,28]. Additionally, there are numerous functional groups that can be substituted into the benzimidazole's seven positions, leading to compounds that have a diverse spectrum of pharmacological activities that affect a number of biological targets [29,30]. Researchers paid close attention to benzimidazole

and its derivatives because of its potential as chemotherapeutics [31]. A variety of therapeutic properties of benzimidazole derivatives, including anticonvulsant [32], antiviral [33], anti-inflammatory [34], urease inhibition [35], anti-oxidant [36], and antidiabetic [37], have been reported. Additionally, oxadiazole is an important heterocyclic molecule containing two nitrogen atoms and one oxygen atom arranged in a five-membered ring structure [38]. The presence of the 1,3,4-oxadiazole ring (Fig.1 (b)) significantly impacts the physicochemical and pharmacokinetic properties of the entire molecule. In pharmaceutical chemistry, the 1,3,4-oxadiazole ring is gaining attention as a bioisostere for carbonyl-containing compounds, such as esters, amides, and carboxylic acids [39].

Three-dimensional quantitative structure-activity relationships (3D-QSAR) are regarded as one of the most important techniques in pharmaceutical chemistry [40-42]. This method plays a vital role in predicting how the structure of a molecule relates to its biological activity, enabling the design of more effective drugs [43-45]. It's similar to the approach used in local Moroccan herbal medicine, where the specific properties of plants are studied to understand their effects on health, but here it's done using advanced computational models to predict drug behavior. Comparative molecular field analysis (CoMFA) [46] and comparative molecular similarity indices analysis (CoMSIA) [47] are two widely recognized methods frequently applied in 3D-QSAR molecular modeling to pinpoint the primary structural factors that affect biological activity [48]. Molecular docking is a computational technique used to predict how a small molecule, such as a drug candidate, binds to a target molecule, typically a protein or enzyme [49-51]. The main objective of molecular docking is to determine the optimal orientation and conformation of a ligand (small molecule) as it binds to the active site of a receptor (protein) [52,53]. ADMET properties refer to the Absorption, Distribution, Metabolism, Excretion, and Toxicity characteristics of a drug candidate. These properties are crucial in drug development as they determine the drug's behavior in the human body and its overall effectiveness and safety [54]. Understanding ADMET properties helps in predicting the pharmacokinetic and pharmacodynamic profiles of compounds, ensuring they reach the intended target and perform their function without causing harm [55,56].

In this study, 20 benzimidazole-based oxadiazole molecules were sourced from the literature [7]. These compounds were synthesized by Taha et al. through straightforward methods and readily available substrates [7]. The 3-methyl-ophenylenediamine was reacted with methyl-4-formyl benzoate in the presence of $\text{Na}_2\text{S}_2\text{O}_5$ in DMF as solvent and the reaction mixture was refluxed for 6 hours to give the benzimidazole ester (i). The benzimidazole ester intermediate (i) was first reacted with hydrazine hydrate in ethanol and refluxed for six hours, resulting in benzimidazole hydrazide (ii). Subsequently, benzimidazole hydrazide (ii) was reacted with different aromatic aldehydes. The reaction mixture was acidified by adding 3-4 drops of acetic acid and refluxed for three hours to

yield the intermediate N'-benzylidene-4-(7-methyl-1H-benzo[d]imidazol-2-yl) benzohydrazide (iii). Finally, the intermediate (iii) underwent oxidative cyclization with phenyliodoacetate as the oxidizing agent in DCM, and the reaction mixture was stirred at room temperature to produce the targets molecules (1-20) (Fig.2) [7].

This research aims to investigate the structure-activity relationship of 20 benzimidazole-based oxadiazole molecules to pinpoint key regions that enhance or reduce α -glucosidase inhibitory activity. Based on these findings, new candidate molecules with promising activity were proposed. These newly suggested compounds were analyzed using various in silico techniques, including molecular docking, molecular dynamics simulations, and DFT calculations.

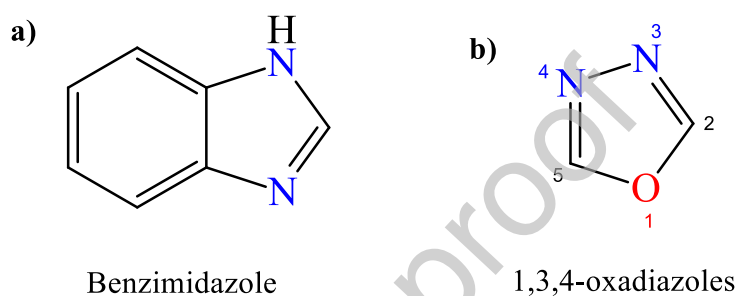


Fig. 1. Chemical structure of benzimidazole (a) and 1,3,4-oxadiazole (b) molecules.

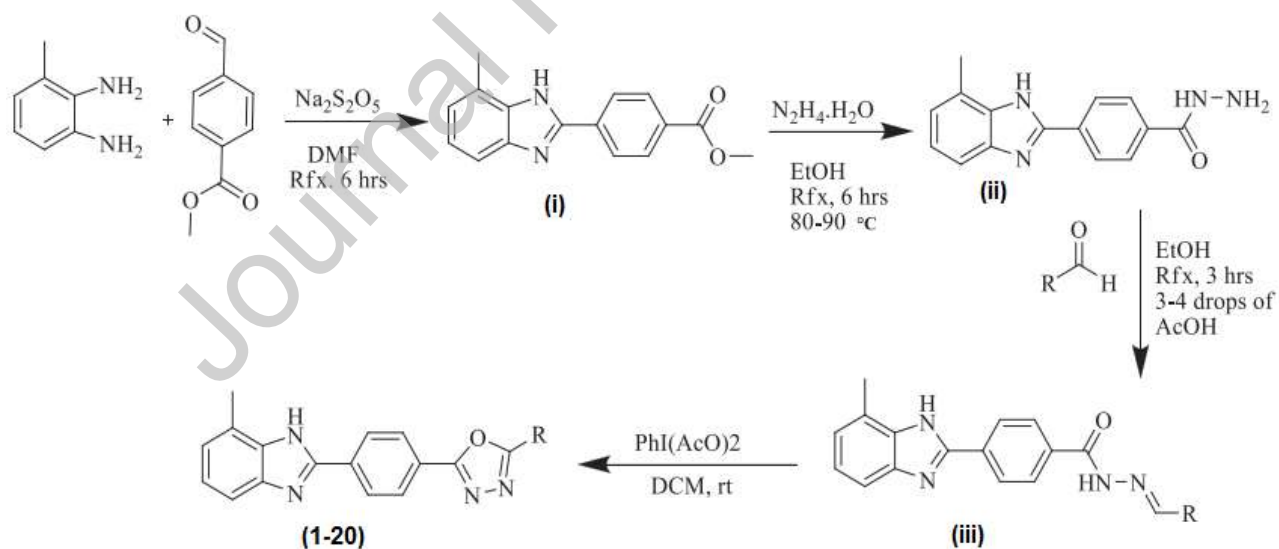


Fig. 2. Synthesis of benzimidazole based oxadiazole derivatives (1-20) [7].

Materials and Methods

Data collection

On the basis of the experimental study, twenty benzimidazole-based oxadiazole molecules identified as α -glucosidase inhibitors were selected for molecular modeling [7]. These molecules were split into two groups; a training set of 16 randomly selected molecules is used to shape the model, while a test set of 4 molecules is preserved to assess the model's accuracy. To perform a 3D-QSAR model, the experimental α -glucosidase activities IC_{50} were converted into the equivalent pIC_{50} values using the following formula $pIC_{50} = \log_{10}(IC_{50})$. The chemical structures of the twenty benzimidazole-based oxadiazole inhibitors and their corresponding pIC_{50} activity values are displayed in Fig. 3 and Table 1.

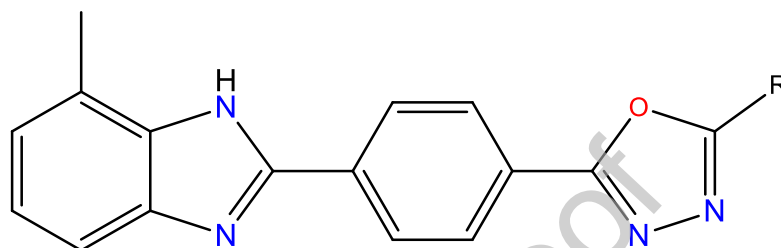

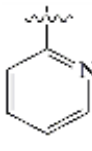
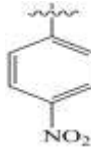
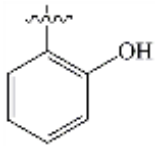
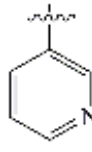


Fig. 3. The general structure of the investigated derivatives.

Table 1. Chemical structures and α -glucosidase activities of benzimidazole-based oxadiazole compounds.

N ^o	R	pIC_{50}	N ^o	R	pIC_{50}	N ^o	R	pIC_{50}
1		5.337	8		3.854	15		4.309
2*		5.022	9*		4.493	16		4.614
3		5.585	10		4.535	17		4.415
4		4.719	11		4.199	18		4.442
5		4.845	12*		5.032	19		4.609

6		4.595	13		4.717	20		4.249
7		4.740	14*		4.143	<i>*Test set molecules</i>		

Database minimization and alignment technique

Molecular alignment is a crucial step adopted to implement 3D-QSAR molecular modeling before building a model. Practically, each of the 20 benzimidazole-based oxadiazole molecules' structures was sketched and optimized using the Tripos force field [57], Gasteiger Huckel charges [58], and gradient convergence criteria of 0.005 kcal/mol. Then, they were aligned on a common core using the ALIGN DATABASE method available in SYBYL-X 2.0 program (Fig. 4). Molecule C3, the most active compound in the database, was selected as the template for this study.

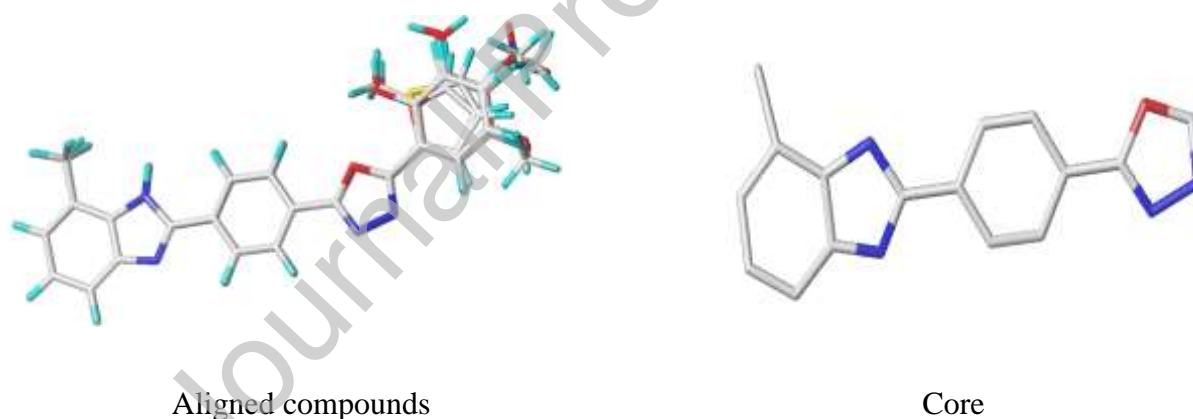


Fig. 4. The alignment and overlap of the data set using compound C3 as a model.

CoMFA and PLS analysis

The CoMFA [46] model was constructed using the partial least squares (PLS) technique based on the chemical structures and α -glucosidase inhibitory activity of training set. The CoMFA steric and electrostatic fields were determined using the Tripos force field [57] with a distance-dependent dielectric constant at each lattice intersection of a variant grid spaced 0.5-3.0Å apart. The default value of 30 kcal/mol was set for the energy cutoff computations. On the other hand, the PLS [59] approach using the leave-one-out (LOO) cross-validation with a column filtering value of 2.0 kcal mol⁻¹ was conducted to provide the cross-validated coefficient Q^2 and optimal

number of components (N). Then, using non-cross-validation, the PLS approach was redone to obtain the determination coefficient R^2 , standard error of estimate (SEE) and F-values.

CoMSIA analysis

CoMSIA [47] technique is wealthier than CoMFA in term of structural geometric that used to compute the similarity indices. As a matter of fact, CoMSIA approach was accomplished in this part to identify the hydrophobic, hydrogen bond acceptor and donor fields along with the electrostatic and steric fields. So, CoMSIA models were molded employing the same indicators which are employed in CoMFA analysis as probe atoms, charge and grid spacing sets.

External Validation of 3D-QSAR Model

A study by Golbraikh and Tropsha suggests that cross-validation is necessary but not enough to check the predictive capability of the nominated QSAR model [60]. However, an external validation using a set of tests molecules can provide a guarantee of the predictive potential of the molded model. In fact, to assess the predictive capability of the model, the predictive correlation coefficient (R^2_{pred}) was identified using the formula (1) [60]:

$$R^2_{pred} = 1 - \frac{PRESS}{SD} \quad (1)$$

Where the PRESS parameter refers to the squared deviations between the calculated and observed activity values of the compounds in the test set, and the SD parameter represents the squared deviations between the average activity values of the training set and the activity values of the test set.

Furthermore, Golbraikh and Tropsha [60] determined additional statistical factors including the squared correlation coefficients r_0^2 and $r_0'^2$, and the slopes k and k' for an additional statistical analysis regarding the external validation. These parameters were computed using the equations (2), (3), (4), and (5), respectively:

$$r_0^2 = 1 - \frac{\sum(Y_{pred/test} - k \times Y_{pred/test})^2}{\sum(Y_{pred/test} - k \times \bar{Y}_{pred/test})^2} \quad (2)$$

$$r_0'^2 = 1 - \frac{\sum(\bar{Y}_{pred/test} - k \times \bar{Y}_{pred/test})^2}{\sum(Y_{pred/test} - k \times Y_{pred/test})^2} \quad (3)$$

$$k = \frac{\sum(Y_{test} \times Y_{pred/test})^2}{\sum(Y_{pred/test})^2} \quad (4)$$

$$k' = \frac{\sum(Y_{pred/test} \times Y_{test})^2}{\sum(Y_{test})^2} \quad (5)$$

An investigation carried out by Roy [61] demonstrated that it is compulsory to calculate the parameters r_m^2 and $r_m'^2$, which are the distinction between r^2 and r_0^2 values, r^2 and $r_0'^2$ values, respectively to ensure the efficiency of the model and thus could be considered for the prediction of the activity of newly put forward compounds. r_m^2 and $r_m'^2$ parameters are calculated using the expressions (6), and (7), respectively:

$$r_m^2 = r^2 \left(1 - \sqrt{(r^2 - r_0^2)} \right) \quad (6)$$

$$r_m'^2 = r^2 \left(1 - \sqrt{(r^2 - r_0'^2)} \right) \quad (7)$$

Y-Randomization Test

The Y-randomization is another validation method employed to determine the model's strength [62]. In fact, the approach was to randomly permute the pIC_{50} values in the training set and then a new model was established after each permutation. The Q^2 and R^2 values that are lower than the original model demonstrate the high capacity of the recommended models. While high values indicate the weakness and fallibility of the models. Hence, the goal of this test is to eliminate any chance of coincidence.

New benzimidazole-based oxadiazole derivatives Design and Activity Prediction

The primary objective of this research is to design novel α -glucosidase inhibitors with important inhibitory activity. To achieve this goal, the CoMFA/CoMSIA model was constructed, validated, and subsequently employed to generate CoMFA /CoMSIA contribution and contour maps. These maps offer valuable understandings regarding the structural characteristics and regions that significantly influence the inhibitory activity of the designed compounds, aiding in the rational design and optimization of new potential inhibitors. The newly designed molecules underwent sketching, minimization, and alignment using the same procedure as the seventeen previously studied molecules. The α -glucosidase activity of the newly designed benzimidazole-based oxadiazole molecules was forecasted using the most reliable and well-established CoMFA /CoMSIA model.

ADME/Tox Prediction

ADME/Tox (absorption, distribution, metabolism, excretion, and Toxicity) prediction has emerged as a fundamental and extensively employed approach in molecular modeling to assess the pharmacokinetic characteristics of molecules [9]. This predictive tool plays a crucial role in understanding how a compound is absorbed, distributed, metabolized, and eliminated in the body,

on top of its possible toxicity [1]. It aids in the initial phases of drug discovery and development by providing valuable information about a molecule's behavior within the human body, facilitating the identification of potential drug candidates with favorable ADME/Tox profiles. Keeping this in mind, we used pkCSM [63] and SwissADME [64] online servers to predict the ADME/Tox parameters of the newly designed candidate scaffolds.

Molecular docking study

Molecular docking was carried out using Autodock Vina [65] program in order to examine the different interactions between ligands and receptor. The protein data bank online site was used to generate the crystal structure of isomaltase from *Saccharomyces cerevisiae* with PDB ID: 3a4a [1,66] and a resolution of 1.60 Å. The water molecules and all the ligands located in 3a4a protein were eliminated using Discovery Studio 2016 program [67]. The active site of the enzyme has been clearly identified, with its precise coordinates measured at $x = 21.595$, $y = 7.436$, and $z = 24.042$. A box grid was established within the pocket of the 3A4A receptor, extending in the directions of $x = 30$, $y = 30$, and $z = 30$. This grid features a spacing of 1 Å between the grid points, allowing for precise mapping of potential interactions and facilitating molecular docking studies within the active site. In the AutoDock 1.5.6 tools, an advanced file format known as PDBQT is utilized for coordinate files, which incorporate essential details such as atomic partial charges and atom types. This format enhances the representation of molecular structures, allowing for more accurate simulations. Additionally, the flexibility of ligands and their non-bonded rotations are specified using torsion angles, enabling detailed exploration of ligand-receptor interactions during docking studies. The most active molecule in the dataset (compound C3), along with the newly proposed compounds, was docked to explore potential interactions with the studied 3a4a receptor. The produced outcomes were examined using Discovery Studio 2016 [67] software.

Molecular dynamics (MD) simulations

The stability of protein-ligand interactions between benzimidazole-based oxadiazole derivatives and 3a4a protein was assessed using molecular dynamics (MD) simulations. The best docking poses obtained by AutoDock-Vina were used for MD simulations using Schrodinger's Maestro Suite 2018-4 [68]. The preparation of the molecular system involved several key steps. Bond orders were assigned, zero-order bonds were created for metals, and disulfide bonds were formed. Water molecules were added outside a 0.00 Å radius, and ionization states were adjusted at a pH of 7 using Epik. During the refinement phase, optimization steps included adjusting water orientations, minimizing hydrogens in modified species using the PRPKA model at pH 7 to

account for ionic effects, and performing additional minimization to remove poorly solvated water molecules and achieve convergence of heavy atoms to an RMSD of 0.3 Å. Hydrogens were selectively added to optimize hydrogen interactions, and the OPLS3e force field was applied for precise atomic interactions. The system was set up orthorhombically with dimensions a, b, and c at 10 Å to minimize volume, and ions were added to maintain a 0.15 M NaCl concentration [69]. The simulations were run for 200 ns, with trajectory data recorded every 4.8 ps and energy data every 1.2 ps, resulting in approximately 50,000 frames. The simulation ensemble was configured for Normal Pressure and Temperature (NPT) at 300 K and 1.01325 bar pressure. A pre-simulation relaxation process ensured that the system began from a stable configuration, providing reliable dynamics throughout.

Density Functional Theory (DFT) Analysis

DFT plays a crucial role in drug design, particularly in the initial phases of drug development, where understanding the molecular properties and interactions of potential drug candidates is essential [70]. DFT offers a powerful computational framework for investigating the electronic structure of molecules, making it highly valuable for rational drug design. In this study, three selected benzimidazole-based oxadiazole compounds were studied in depth using the DFT approach. DFT calculations of these molecules were conducted using the Gaussian G09 software package [71] on the basis of B3LYP/6-31G (d,p) in order to reach the equilibrium geometry of each compound and determine the reactivity indices. Molecular Electrostatic Potential (MEP) is an appreciated tool for investigating the charge distribution within a molecule, providing a visual representation of how different regions of a molecule interact with electrostatic forces. It is commonly employed in drug design and computational chemistry to understand how a molecule might interact with other molecules, such as biological targets, by examining its surface properties [72].

Results and Discussion

CoMFA and CoMSIA results

The 3D-QSAR models were molded based on the combination between CoMFA/CoMSIA descriptors and α -glucosidase inhibitory activity. The statistical parameters characterizing the models are listed in Table 2. The observed and calculated pIC_{50} values along with their residuals are revealed in Table 3.

Results of Table 2 demonstrate that produced CoMFA model has good value of Q^2 (0.594), significant value of R^2 (0.958), small SEE value (0.1), four optimum number of components, and F value of 62.478. Additionally, the CoMFA model's competence was tested using an external

validation method, and the R^2_{test} result was 0.850. Therefore, the established CoMFA model has good robustness. On the other hand, the CoMFA model composed of two fields; the steric and electrostatic contributions are 0.607 and 0.393, respectively; demonstrating that the importance of the steric field exceeds that of the electrostatic.

Regarding the CoMSIA model, different combinations using the steric (S), electrostatic (E), hydrophobic (H), hydrogen bond acceptor (A) and donor (D) fields were made to generate numerous CoMSIA models (Table 2). Taking into account the top values of Q^2 , R^2 and R^2_{test} , the CoMSIA/SED model was selected. We can see from Table 2 that CoMSIA/SED model has good value of Q^2 (0.616), important value of R^2 (0.928), small value of SEE (0.125) and good value of N (3). The CoMSIA/SED model was also verified for its external power; the obtained R^2_{test} was 0.63. Moreover, the steric, electrostatic and hydrogen bond donor contributions were 0.061, 0.507 and 0.432 ratios, respectively. As a result, the hydrogen bond donor and electrostatic moieties will have more effect on the activity of the benzimidazole-based oxadiazole inhibitors.

The results of Table 3 strongly indicated that the residual between the estimated and real pIC_{50} activities is not exceeding 1 logarithmic unit. Therefore, any molecule among the twenty benzimidazole-based oxadiazole derivatives was regarded as outlier.

The graphs of CoMFA and CoMSIA/SED models using the observed and calculated pIC_{50} values of the twenty benzimidazole-based oxadiazole molecules are presented in Fig. 5. The strong linear relationships demonstrated that the α -glucosidase activities predicted by the recommended models are in accord with those of the experiment; revealing the CoMFA and CoMSIA/SED models' excellent proficiency.

Table 2. Statistical parameters of the developed CoMFA and CoMSIA models.

Model	Q^2	R^2	SEE	F	N	R^2_{test}	Fractions				
							Ster	Elec	Acc	Don	Hyd
CoMFA	0.600	0.958	0.100	62.478	4	0.72	0.607	0.393	-	-	-
CoMSIA/SED	0.616	0.928	0.125	51.424	3	0.63	0.061	0.507	-	0.432	-
CoMSIA/SHD	0.794	0.965	0.091	76.657	4	0.56	0.178	-	-	0.574	0.248
CoMSIA/EHD	0.564	0.932	0.122	54.445	3	0.22	-	0.515	-	0.402	0.082
CoMSIA/SEDA	0.510	0.924	0.134	33.468	4	0.55	0.053	0.433	0.208	0.305	-
CoMSIA/SEHD	0.640	0.954	0.104	57.360	4	0.53	0.055	0.437	-	0.425	0.083
CoMSIA/SEHDA	0.537	0.948	0.111	49.777	4	0.54	0.048	0.388	0.203	0.291	0.071

R^2 : Non-cross-validated correlation coefficient; SEE: Standard error of the estimate; Q^2 : Cross-validated correlation coefficient; F: F-test value; N: Optimum number of components; R^2_{test} : External validation correlation coefficient.

Table 3. Observed and predicted α -glucosidase activity as well as their residual of the 20 studied molecules.

N ^o	pIC ₅₀	CoMFA		CoMSIA/SED	
		Predicted	Residuals	predicted	Residuals
1	5.337	5.318	0.019	5.437	-0.100
2*	5.022	5.171	-0.149	5.035	-0.013
3	5.585	5.431	0.154	5.428	0.157
4	4.719	4.737	-0.018	4.719	0.000
5	4.845	4.912	-0.067	4.808	0.037
6	4.595	4.786	-0.191	4.796	-0.201
7	4.740	4.737	0.003	4.588	0.152
8	3.854	3.742	0.112	3.918	-0.064
9*	4.493	4.437	0.056	4.618	-0.125
10	4.535	4.588	-0.053	4.623	-0.088
11	4.199	4.197	0.002	4.086	0.113
12*	5.032	4.917	0.115	4.819	0.213
13	4.717	4.621	0.096	4.612	0.105
14*	4.143	4.339	-0.196	4.351	-0.208
15	4.309	4.253	0.056	4.319	-0.010
16	4.614	4.58	0.034	4.461	0.153
17	4.415	4.502	-0.087	4.536	-0.121
18	4.442	4.451	-0.009	4.563	-0.121
19	4.609	4.569	0.040	4.590	0.019
20	4.249	4.330	-0.081	4.273	-0.024

*Test set molecules

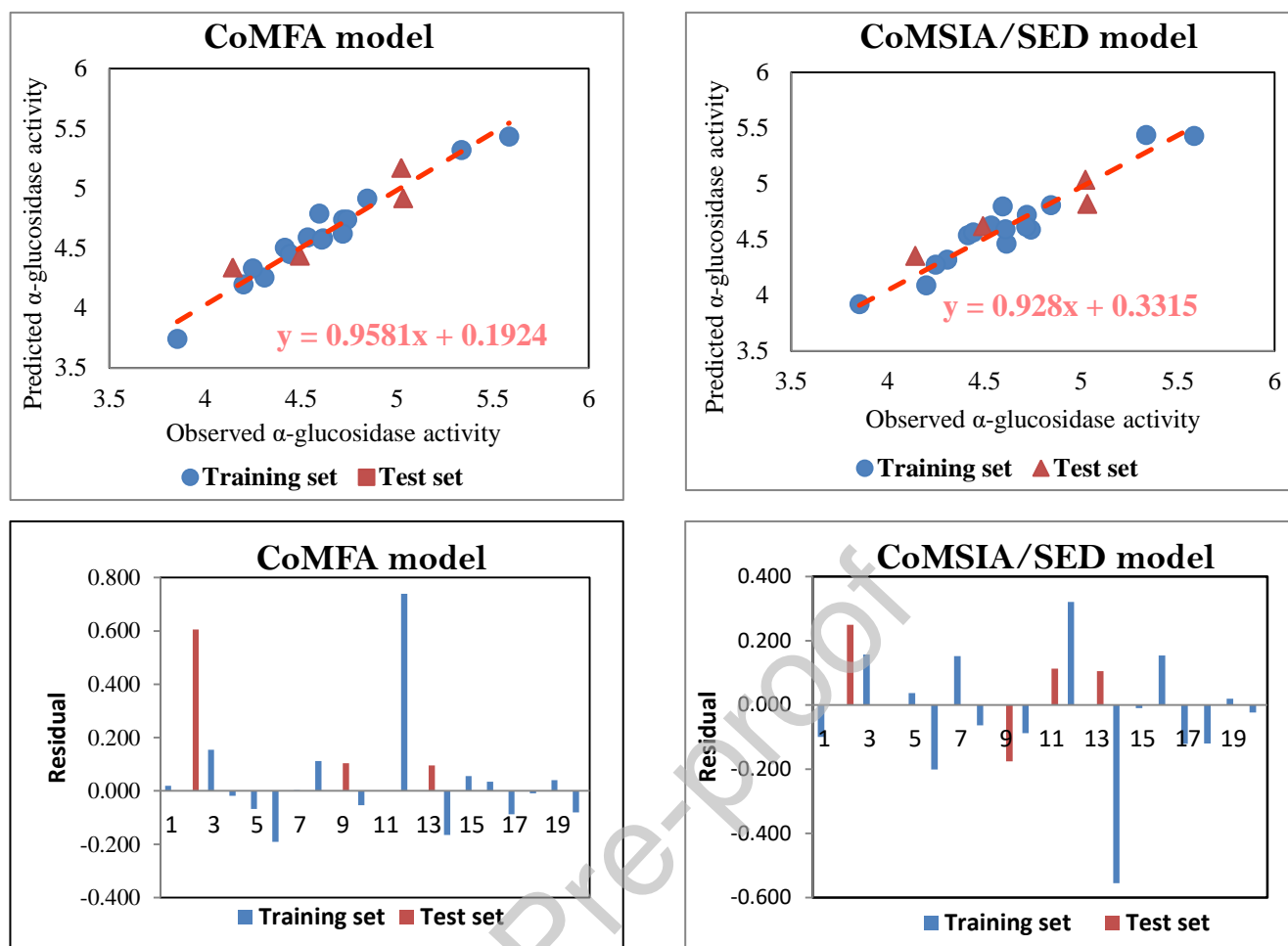


Fig. 5. Predicted and observed pIC_{50} plots of the investigated molecules along with their residuals using the CoMFA and CoMSIA/ SED models.

Validation of 3D-QSAR Models

To ensure the reliability of the predicted 3D-QSAR models, an external validation using the Golbraikh and Tropsha criteria, as well as the Roy criterion, was carried out. Four benzimidazole-based oxadiazole derivatives were used for this technique and the obtained results are listed in Table 4.

The data in Table 4 reveals that the CoMFA and CoMSIA/SED models consistently deliver reliable outcomes, as they adhere to the Golbraikh and Tropsha parameters, confirming their compliance with the established criteria. Furthermore, the r_m^2 and $r_m'^2$ values for the CoMFA and CoMSIA/SED models are 0.59 and 0.63, and 0.584 and 0.617, respectively—each surpassing the 0.5 threshold. Additionally, the models demonstrate a Δr_m^2 value below 0.2 and a Δr_0^2 value that does not exceed 0.3. Consequently, both the CoMFA and CoMSIA/SED models have successfully fulfilled the Roy criterion requirements. The CoMFA and CoMSIA/SEDA models, chosen as the preferred models,

exhibited exceptional reliability and stability in external validation tests. Consequently, there is strong confidence in their ability to accurately predict the α -glucosidase activity of potential new molecules.

Table 4. External validation results of the CoMFA and CoMSIA/SEDA models using Golbraikh, Tropsha, and Roy criteria

Criteria	Parameter	Validation Criteria	CoMFA	CoMSIA/SED
Golbraikh and Tropsha	r_0^2	$r_0^2 > 0.5$	0.984	0.988
	$r_0'^2$	$r_0'^2 > 0.5$	0.989	0.996
	r^2_{pred}	$r^2 > 0.6$	0.877	0.898
	k	$0.85 \leq k \leq 1.15$	0.990	0.994
	$\frac{r^2 - r_0^2}{r^2}$	< 0.1	-0.121	-0.099
	k'	$0.85 \leq k \leq 1.15$	1.008	1.004
	$\frac{r^2 - r_0'^2}{r^2}$	< 0.1	-0.127	-0.108
Roy	r_m^2	$r_m^2 > 0.5$	0.590	0.630
	$r_m'^2$	$r_m'^2 > 0.5$	0.584	0.617
	Δr_m^2	$\Delta r_m^2 < 0.2$	-0.006	-0.012
	Δr_0^2	$\Delta r_0^2 < 0.3$	-0.005	-0.009

Y-randomization result

Y-randomization validation was conducted to evaluate the reliability of the recommended models, with the results presented in Table 5. The results indicate that the Q^2 and R^2 values for the CoMFA and CoMSIA/SED models are reduced compared to those of the original models. As a result, the selected models are robust and their predictive power is not due to chance correlations.

Table 5. Q^2 and R^2 values of the constructed models following Y-randomization tests.

Iteration	CoMFA		CoMSIA/SED	
	Q^2	R^2	Q^2	R^2
1	-0.488	0.900	-0.084	0.750
2	-0.224	0.913	-0.126	0.763
3	-0.271	0.920	-0.183	0.759
4	-0.135	0.919	-0.130	0.746
5	-0.097	0.932	-0.065	0.762
Original model	0.600	0.958	0.616	0.928

CoMFA contour map result

The molded CoMFA model was used to produce the CoMFA contour maps in order to explain the effect of steric and electrostatic groups on the α -glucosidase inhibitory activity of benzimidazole-based oxadiazole inhibitors. The results obtained are presented in Fig. 6.

According to CoMFA steric contour maps, the green colored portion around *meta* hydroxyl moiety of the benzene-1,2-diol moiety points out that massive moiety might enhance the activity of the benzimidazole-based oxadiazole entities (Fig. 6 (a)).

The red colored portions cover 1,3,4-oxadiazole, around 1,2-diol moieties, *meta* position of the benzene-1, 2-diol group suggest that substituents with electro-withdrawing character might improve the α -glucosidase activity of the molecules (Fig. 6 (b)). These results provide insights into how the structural features of benzimidazole-based oxadiazole compounds relate to their α -glucosidase activities. By analyzing specific structural elements, such as functional groups and molecular conformations, we can better understand their influence on activity levels. This relationship is crucial for guiding the design of more effective inhibitors, as it highlights which structural modifications may enhance or diminish the compounds' efficacy in inhibiting α -glucosidase, ultimately contributing to more targeted therapeutic strategies.

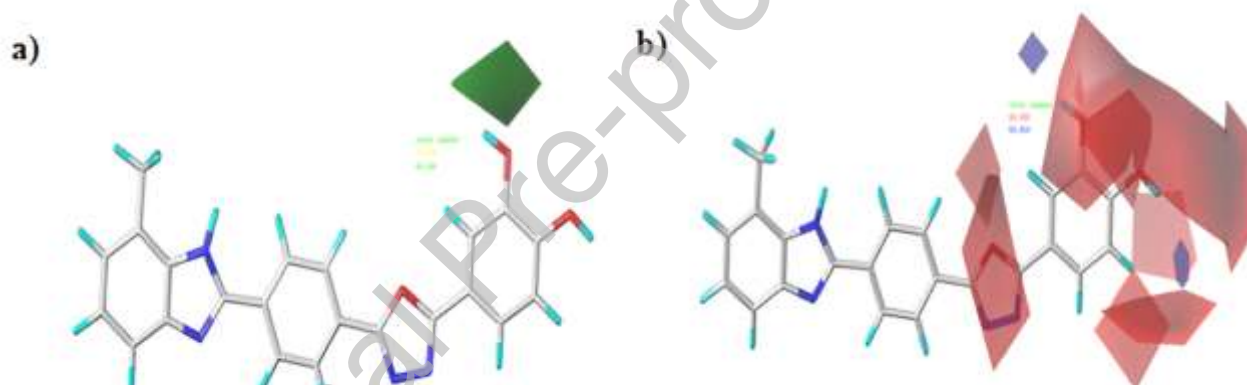


Fig. 6. Contours maps results obtained from CoMFA developed model. a) Steric and b) Electrostatic.

CoMSIA/SED Contour Map

CoMSIA/SED contour maps were constructed to elucidate the effect of steric, electrostatic and hydrogen bond donor moieties on the α -glucosidase inhibitory activity of benzimidazole-based oxadiazole inhibitors and the findings obtained are showed in Fig. 7.

As demonstrated in Fig. 7 (a), the huge green contours around the hydroxyl group situated in *para* position of the phenyl part, *ortho* and *meta* places of the benzene-1,2-diol suggest that substituents with steric effects are required to ameliorate the α -glucosidase inhibitory activity of benzimidazole-based oxadiazole molecules.

In the Fig. 7 (b), the red contour around *meta* hydroxyl group of the benzene-1, 2-diol demonstrates that electron-withdrawing substituents might enhance the activity of the molecules. On the other side, the blue colored portion about *para* position of the phenyl moiety points out that group with electron-withdrawing character in this position is unflavored. The last finding may explain why some molecules in the dataset. For example, the molecule 20 ($pIC_{50} = 4.249$), which has an electron-withdrawing substituent in the *para* position of the benzene-1,2-diol moiety, has decreased α -glucosidase activity.

In Fig. 7 (c), the large purple part covering *meta*, *para* and *ortho* sites of the benzene-1,2-diol moiety elucidates that these positions are earmarked only for hydrogen bond acceptor moieties to ameliorate the α -glucosidase inhibitory activity.

In conclusion, we have compiled all the CoMFA and CoMSIA/SED contour maps, which will serve as a valuable resource for identifying the structural features that influence the α -glucosidase inhibitory activity of the compounds (Fig. 8). Consequently, this analysis will facilitate the development of new benzimidazole-based oxadiazole inhibitors with enhanced inhibitory efficacy, ultimately contributing to more effective treatments for conditions such as diabetes mellitus. By leveraging these findings, we aim to propose optimized compounds that can significantly improve therapeutic outcomes.

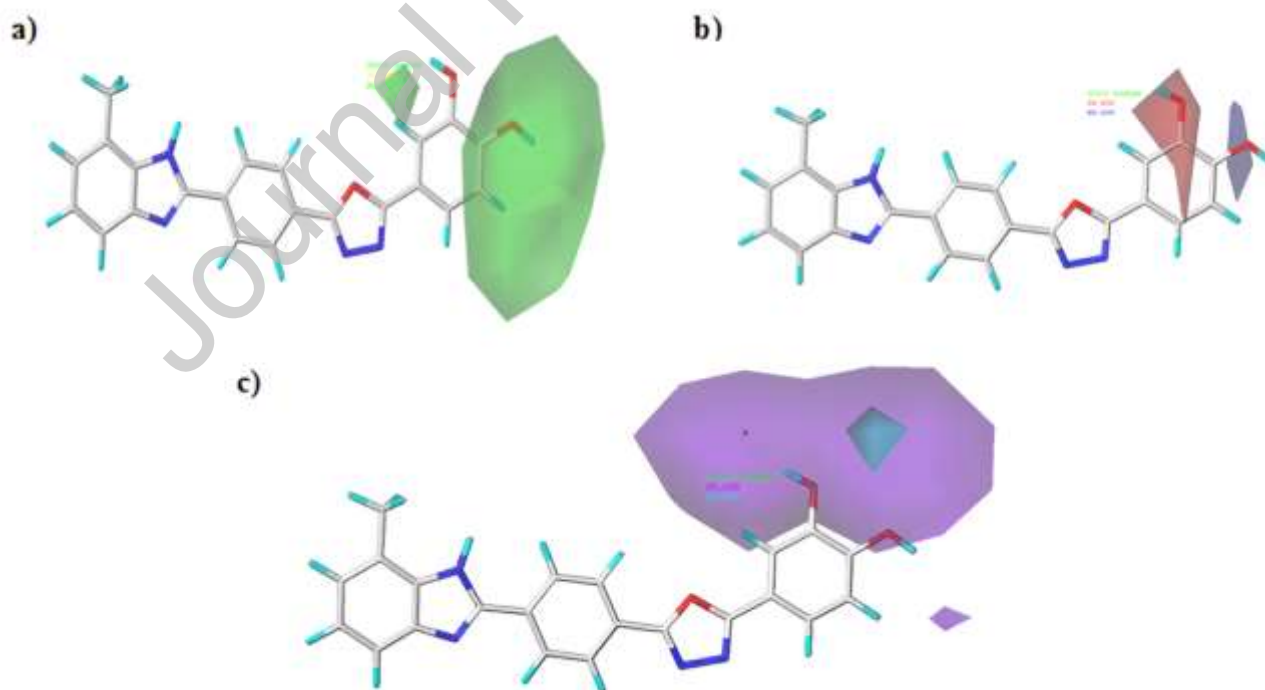


Fig. 7. CoMSIA/SED contours maps results. a) steric, b) electrostatic, c) H-bond donor.

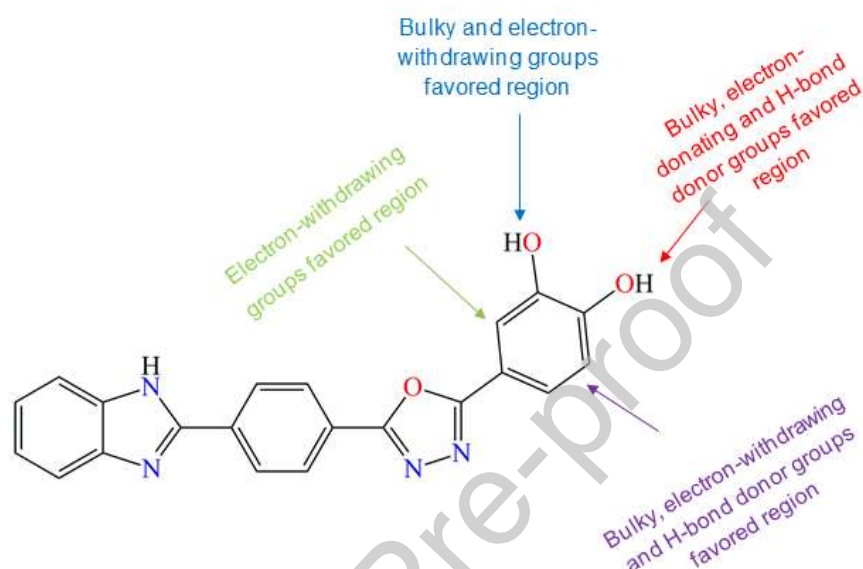
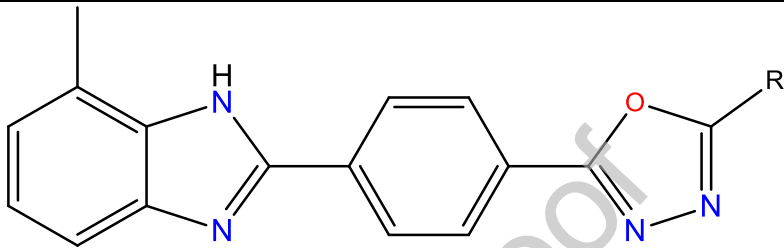

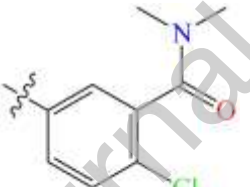
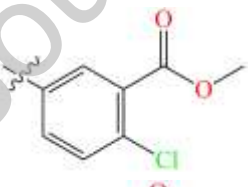
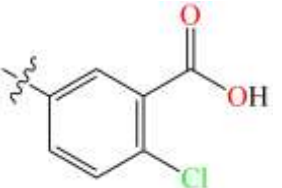


Fig. 8. Structural requirements for α -glucosidase activity obtained from CoMFA and CoMSIA/SED contour maps.

Design of new benzimidazole-based oxadiazole derivatives

The effective interpretation of the CoMFA and CoMSIA/SED contour maps allows us to identify specific moieties that could enhance α -glucosidase inhibitory activity. By understanding these relationships, we successfully designed four potent benzimidazole-based oxadiazole inhibitors. Their activities were then evaluated using the most reliable CoMFA and CoMSIA/SED models, as detailed in Table 5. This rigorous approach not only highlights the potential of these new inhibitors but also underscores the importance of structure-activity relationships in guiding medicinal chemistry efforts. The insights gained from these models will aid in optimizing the inhibitors further, paving the way for their development into effective therapeutic agents. The new benzimidazole-based oxadiazole molecules were sketched, aligned, and minimized using the same route adopted in the total set molecules.

Table 6. Chemical structure of new α -glucosidase inhibitors and their predicted pIC_{50} values

Based structure			
			
N°	Structure	Predicted pIC_{50}	
	R	CoMFA	CoMSIA/SED
M1		5.10	6.77
M2		4.96	6.76
M3		5.13	6.27
M4		5.11	5.86

Drug-likeness outcomes

Drug-likeness refers to the properties of a chemical compound that make it likely to become an effective drug. It describes whether a compound has the characteristics necessary for optimal

interaction with biological systems while having favorable pharmacokinetics and safety profiles. Lipinski's rule of five has been a dominant guideline in this area, stating that molecules with a molecular weight (MW) under 500 Da, a logP value below 5, fewer than 10 hydrogen bond acceptors (HBA), and fewer than 5 hydrogen bond donors (HBD) tend to exhibit optimal oral absorption and permeability [73]. In this context, various molecular properties of the newly proposed benzimidazole-based oxadiazole compounds were evaluated using the pkCSM [63] and SwissADME [64] online tools to determine their Lipinski's properties as shown in Table 7. The data presented in Table 7 suggest that the proposed compounds demonstrate favorable absorption and permeability. Additionally, compounds with a total polar surface area (TPSA) below 140 Å² and no more than 10 rotatable bonds (nrotb) are likely to have acceptable bioavailability and enhanced flexibility, allowing for more effective interaction with a specific binding pocket [18]. As shown in Table 7, the four proposed compounds exhibit good bioavailability and increased flexibility at the receptor's binding site. Additionally, the synthetic accessibility (SA) of the new benzimidazole-based oxadiazole molecules was evaluated to determine their potential for synthesis. The findings in Table 7 revealed that all the molecules have synthetic accessibility values close to 1 and far from 10, indicating that they are easily synthesizable [74]. The findings indicated that the new benzimidazole-based oxadiazole derivatives fully complied with the key rules of drug-likeness, specifically those outlined by Lipinski, Veber, and Egan (Table 8).

Table 7. Lipinski's parameters of the new benzimidazole-based oxadiazole inhibitors.

Inhibitor	Property						
	Log P	HBD	HBA	TPSA	nrotb	MW	SA
M1	5.00	2	5	110.69	4	429.867	3.22
M2	5.61	1	5	87.91	4	457.921	3.39
M3	5.69	1	6	93.90	4	444.878	3.44
M4	5.60	2	5	104.90	4	430.851	3.30

HBD: number of hydrogen bonds donors, **HBA:** number of hydrogen bonds acceptors, **LogP:** logarithm of partition coefficient of compound between n-octanol and water, **TPSA:** Topological Polar Surface Area, **MW:** Molecular Weight, **nrotb:** number of rotatable bonds, **SA:** Synthetic Accessibility

Table 8. Drug likeness prediction of the proposed compounds basing on Lipinski, Veber and Egan rules.

Compound	Rule		
	Lipinski	Veber	Egan
M1	Yes	Yes	Yes
M2	Yes	Yes	Yes
M3	Yes	Yes	Yes
M4	Yes	Yes	Yes

ADME results

The quest for new potent drugs is fraught with challenges, particularly in ensuring that these compounds do not induce unwanted side effects. This is crucial in drug discovery, where the therapeutic index—the ratio between the toxic and therapeutic doses—needs to be maximized. To address these challenges, researchers have increasingly turned to the analysis of pharmacokinetic properties, which encompass absorption, distribution, metabolism, and excretion (ADME) of potential drug candidates. In this part, we determined the ADME properties of newly proposed benzimidazole-based oxadiazole molecules. These compounds were selected due to their promising biological activity. To systematically evaluate their pharmacokinetic profiles, we utilized two robust online tools: pkCSM [63] and SwissADME [64]. The achieved outcomes are listed in Table 9.

The journey of a drug from the site of administration to the site of action is referred to as absorption [50]. For a medication to have any therapeutic effects, it must be absorbed into the bloodstream, which makes absorption a crucial focus in drug development. The findings obtained indicate that the studied benzimidazole-based oxadiazole molecules present high absorption. Regarding the water solubility; outcomes of Table 9 show that the four recommended inhibitors are soluble in water. Because high permeability would translate into a predicted value greater than 0.9, the Caco-2 permeability results show that the predicted molecule M3 cannot enter Caco-2 [51]. All four proposed derivatives were found to be substrates and inhibitors of P-glycoprotein (Table 9). Additionally, the blood brain barrier (BBB) can be defined as the primary barrier separating the circulatory system and the central nervous system. It is a crucial characteristic that determines whether a drug may breach the blood-brain barrier and have an impact on the brain [49]. Practically, a chemical is considered to have high brain distribution if $\log_{BB} > -1$ [49]. Subsequently, the BBB permeability founded in Table 9 revealed non-penetrating BBB for the compounds **M2**, **M1** and **M4**. The CYP3A4 enzyme is considered the most important enzyme in the CYP family, responsible for metabolizing 50% of all drugs on its own [50]. According to the findings of table 5, the compounds **M1** and **M2** are substrates and inhibitors of CYP3A4. The compound **M1** was found to be a substrate and not an inhibitor of CYP3A4. The compound **M4** is neither a substrate nor an inhibitor of CYP3A4. In a similar vein, clearance is a parameter that describes the relationship between drug concentration in the body and the rate of drug elimination [48]. A lower clearance value indicates that drugs remain in the body for a longer duration. The results presented in Table 9 show that all examined molecules have a low clearance index. The findings from our pharmacokinetic analyses indicate that the newly proposed benzimidazole-based oxadiazole compounds exhibit favorable ADME properties, suggesting their potential as effective candidates for the development of novel inhibitors for diabetes mellitus.

Table 9. ADME prediction of the new suggested α -glucosidase inhibitors

Models		Compounds			
		M1	M2	M3	M4
		Absorption			
Water solubility	Numeric (Log mol/L)	-2.906	-2.893	-2.892	-2.895
Caco-2 permeability	Numeric (log Papp in 10^{-6} cm/s)	1.005	1.165	0.699	1.158
Intestinal absorption (human)	Numeric (% Absorbed)	100	80.107	100	91.189
P-glycoprotein substrate	Categorical (Yes/No)	Yes	Yes	Yes	Yes
P-glycoprotein inhibitor		Yes	Yes	Yes	Yes
		Distribution			
Blood-brain barrier (logBB)	Numeric (log BB)	-1.523	-1.098	-0.243	-1.715
		Metabolism			
CYP1A2 inhibitor		Yes	Yes	Yes	No
CYP2C9 inhibitor		Yes	Yes	Yes	No
CYP2D6 inhibitor		No	Yes	Yes	No
CYP2C19 inhibitor	Categorical (Yes/No)	Yes	Yes	Yes	No
CYP3A4 inhibitor		No	Yes	Yes	No
CYP2D6 substrate		No	No	No	No
CYP3A4 substrate		Yes	Yes	Yes	No
		Excretion			
Clearance	Numeric (log ml/min/kg)	0.638	0.447	0.641	0.449

Toxicity prediction result

The Ames mutagenicity test is a widely used assay in the initial phases of drug development to evaluate the potential mutagenic effects of a molecule. According to the results presented in Table 10, the proposed molecules M1, M2, M3, and M4 were found to be non-toxic based on the Ames test. Additionally, the proposed molecules did not exhibit any carcinogenicity. Moreover, hepatotoxicity refers to the ability of a substance to cause damage or toxicity to the liver. It is an important aspect of toxicity testing, particularly for drugs and chemicals that are metabolized in the

liver or have the potential to interact with liver cells. From Table 10, we can see that all inhibitors are not hepatotoxic. Additionally, the results hint that the proposed α -glucosidase inhibitors do not exhibit skin sensitisation. Moreover, based on the information provided in Table 10, it appears that the LD50 (lethal dose 50) values of the inhibitors are low. A low LD50 value indicates that a high dosage of the substance would be required to cause lethality in test subjects.

Given the favorable pharmacokinetic properties of the newly proposed compounds, we are poised to advance our research by conducting further studies, specifically molecular docking and molecular dynamics simulations. These computational techniques will provide valuable insights into the binding interactions and dynamic behavior of the compounds with their biological targets.

Table 10. Toxicity prediction of the proposed inhibitors.

Compound	Ames toxicity test	Carcinogenicity	Hepatotoxicity	Skin sensitisation	Oral Rat Acute Toxicity (LD50: mol/Kg)
M1	No-toxic	Non-carcinogen	No-hepatotoxic	No	2.488
M2	No-toxic	Non-carcinogen	No-hepatotoxic	No	2.858
M3	No-toxic	Non-carcinogen	No-hepatotoxic	No	2.831
M4	No-toxic	Non-carcinogen	No-hepatotoxic	No	2.482

Molecular docking results

Molecular docking was conducted to gain a deeper understanding of the binding modes and to investigate the interactions between the synthesized benzimidazole-based oxadiazole derivatives and the 3a4a protein. In this part, compound C3, recognized as the most active molecule among the derivatives evaluated, served as a reference point for comparison. Binding energy and inhibition constant (K_i) values are listed in Table 11. Docking interaction results are presented in Table 12. It can be seen from Table 11 that compounds M1 and M2 have the highest docking score against the receptor, exceeding the docking score of the reference inhibitor, compound C3; suggesting that these compounds have stronger binding affinity and potentially better interaction with the receptor active site compared to compound C3. The inhibition constant (K_i) was determined from the binding energy (ΔG) using the equation $K_i = \exp(\Delta G/RT)$, where R is the universal gas constant ($1.985 \times 10^{-3} \text{ kcal mol}^{-1} \text{ K}^{-1}$) and T is the temperature (298.15 K) [75]. A lower K_i value indicates stronger binding between the drug and the receptor, suggesting higher potency and potentially better therapeutic efficacy. Consequently, compounds M1 and M2 have lower K_i values compared

to compound C3, highlighting their potential as more effective inhibitors of the α -glucosidase receptor. In the visualization of molecular docking interactions, we focus only on compounds M1 and M2 and compare them with compound C3 as reference.

The docking outcome of compound M1 with α -glucosidase receptor demonstrates more types and number of interactions. The amino group formed two conventional hydrogen bond interactions with Lys156 (2.46 Å) and Ser157 (2.97 Å) residues. Conventional hydrogen bond interactions are critically important in drug design, as they play a key role in determining the binding affinity, specificity, and overall effectiveness of a drug. The presence of hydrogen bond interactions in the docking results for compound M1 enhances its potential as an effective α -glucosidase inhibitor, increasing its therapeutic value. The ring of the phenyl moiety which is near to the benzimidazole group forms three different interactions i.e. pi-alkyl, pi-anion and Pi-Pi stacked with Pro312 (4.81 Å), Asp307 (3.47 Å) and His280 (5.01 Å) residues, respectively. The oxadiazole moiety formed Pi-Pi stacked interaction with His280 (4.54 Å) residue. The benzimidazole ring provides pi-alkyl interactions with Val308 (5.33 Å) and Ala329 (4.41 Å) residues (Table 12). These various interactions give to compound M1 a good stability in the active site of 3a4a receptor and validate its predicted inhibitory activity. The docking findings supported the proposed 3D-QSAR models. Moreover, the docking outcome of the compounds M2 presents various interactions with 3a4a receptor as conventional hydrogen bond, carbon hydrogen bond, Pi-sigma, Pi-Pi stacked, Pi-Pi T-shaped (Table 12). These interactions enhance the stability of compound M2 and further strengthen its potential as a lead active compound for targeting diabetes mellitus. On the other hand, compound C3, the most active compound in the data set, interacts very well with the target receptor, providing several types of interactions, mainly conventional hydrogen bonding and the Pi-Pi T-shaped (Table 12). As a conclusion, the results suggest that the new inhibitors M1 and M2 could provide enhanced efficacy and potency in inhibiting the α -glucosidase receptor, positioning them as promising candidates for further development as potential therapeutic agents.

Table 11. Binding energy and inhibition constant (K_i) of new α -glucosidase inhibitors and compound C3.

Compound	Binding energy (Kcal/mol)	Inhibition constant K_i (μ M)
M1	-6.473	0.177
M2	-6.531	0.161
M3	-5.711	0.644
M4	-6.144	0.310
C3	-6.076	0.347

Table 12. 2D and 3D docking visualization of newly designed compounds and compound C3.

Compound	2D diagram	3D diagram
M1		
M2		
C3		

Molecular Docking Validation Result

Re-docking was performed to evaluate and refine the docking procedure and assess its efficiency. The re-docked complex was superimposed onto the co-crystallized native complex, as illustrated in Fig. 9 (a). The resulting RMSD value was 0.35Å. In molecular docking validation, an RMSD value under 2 Å is generally considered indicative of a reliable docking procedure [76]. This low RMSD value demonstrates a high degree of similarity between the re-docked and native complexes, suggesting that the docking model and procedure are robust and accurate in predicting the ligand-binding conformations. Gln279, Arg442, Glu411 and Arg315 are the interacting amino acids formed with an average distance of 3.00 Å in the active site pocket (Fig. 9 (b)).

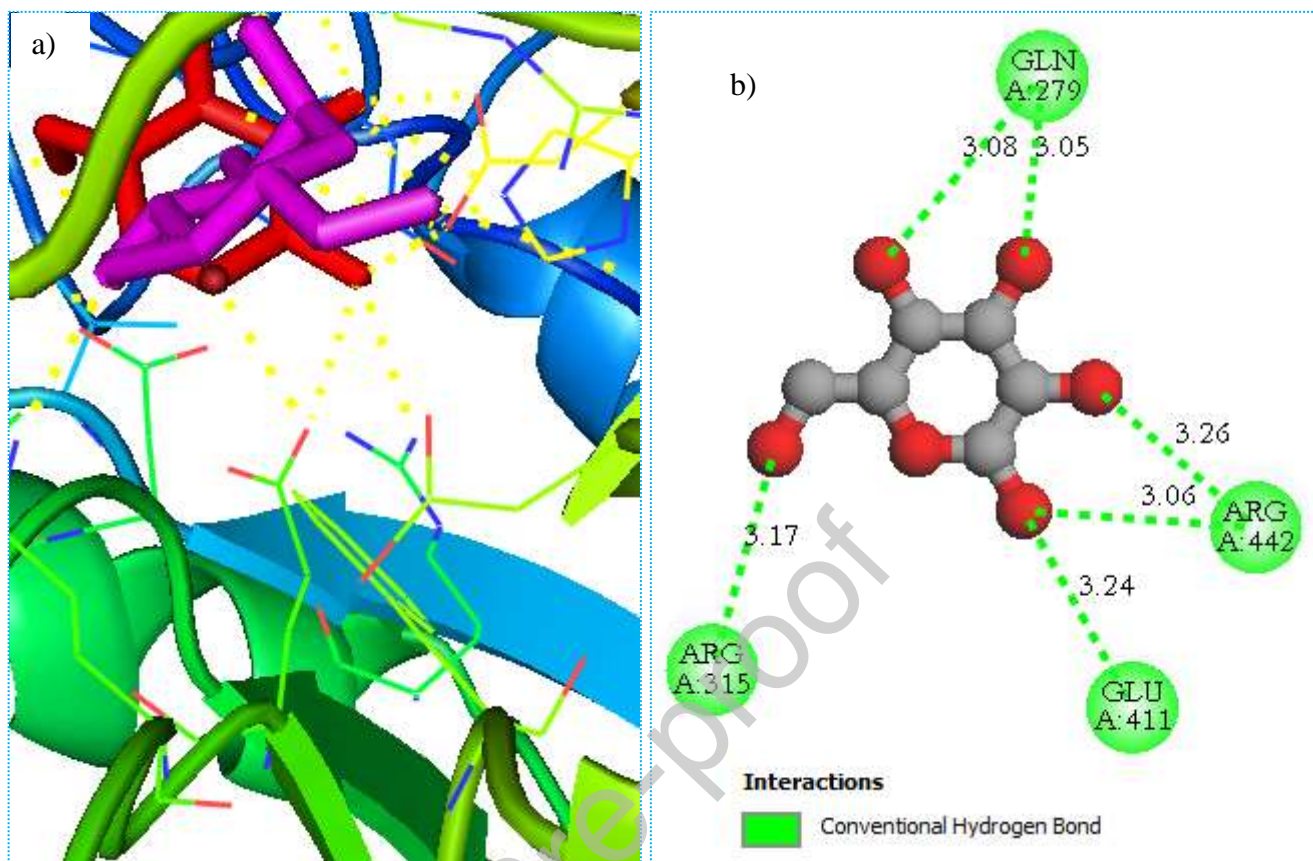


Fig. 9. a) Re-docking pose with the RMSD value of 1.82 Å (Red = Original, Magenta = Docked), b) Docking interactions of the co-crystallized ligand.

MD simulation results

In this section, to compare the structures of the new conformations with the initial structure obtained by molecular docking in the absolute state, an analysis of the RMSD (Root Mean Square Deviation) for the protein (C-alpha), complexes and ligands was performed over 200 ns. Fig. 10 shows the RMSD of the protein without ligand influence (Fig. 10A), complexes (Fig. 10B) and ligands only (Fig. 10C). In the first 25 ns, the RMSD of the protein does not exceed 2 Å following the deviation of the alpha carbons with C3 and M1 ligands, and converges towards an RMSD value of 2.5 Å, except for the C-alpha carbons with M2 ligand, which tends towards an average value of 3 Å. In general, the protein maintains the same conformation after 50 ns and does not exceed 3 Å, indicating the stability of the crystalline structure of the target protein. Regarding the deviation of the C3, M1 and M2 complexes, it is observed that the RMSD of the C3 complex diverges to a maximum value of 8 Å from 120 ns to 140 ns, after which it converges to an RMSD value equal to 6 Å. No stable conformation is observed during 140 ns for the C3 complex. For the other complexes, it is noted that 60 ns is sufficient to stabilize the M1 and M2 complexes, indicating that

the newly designed molecules M1 and M2 form interactions with the therapeutic target that stabilize the complex formed during the dynamic simulation time. Furthermore, the RMSD of the proposed molecules M1 and M2 is always lower than the RMSD of the more active molecule C3. The convergence of the RMSD of the studied complexes M1 and M2 validates the performance of the interactions of the ligands M1 and M2 obtained by the molecular docking method.

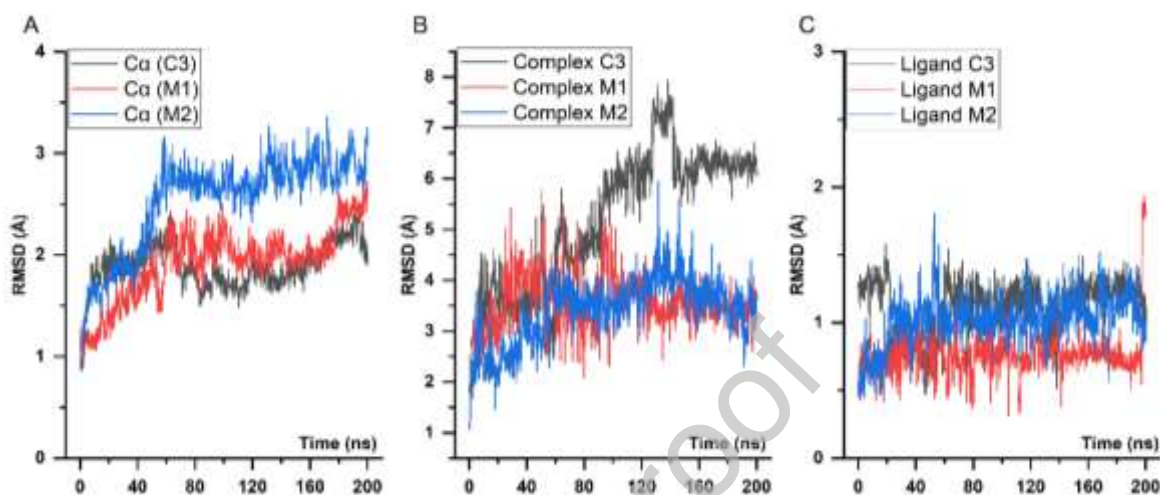


Fig. 10. RMSD of C-alpha (A), complexes (B) and ligands (C).

The protein studied has significant interactions with the C3 ligand, such as hydrogen bonds, as indicated by specific residues such as Lys 156, Ser 157, Tyr 158 and others. These interactions could play a crucial role in the stability and molecular recognition between the protein and its ligand. Analysis of RMSF fluctuations reveals variable dynamics within the protein, with residues showing high values indicating increased flexibility, particularly in regions such as Leu 313. Some residues such as Ser 240, Ser 241, Asp 242 and His 280 show high flexibility, indicating significant mobility. These results suggest significant conformational changes upon interaction with the ligand. In particular, the flexibility of some residues, despite hydrogen bonding, suggests a structural adaptation necessary for efficient binding to the C3 ligand. This in-depth understanding of molecular interactions and protein flexibility may have important implications for drug design or understanding of related biological processes. Fig. 11 shows that the fluctuation of all amino acids in the target did not exceed 3\AA and that these amino acids formed several types of interactions with the C3 ligand.

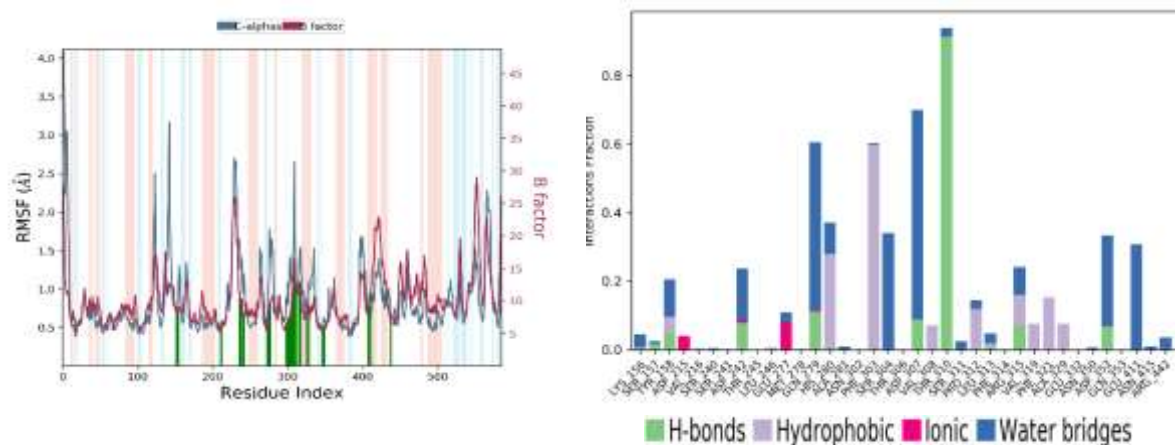


Fig. 11. RMSF of C3 complex amino acids, H-Bonds and fractions of each interaction.

Analysis of the RMSF results (Fig. 12) and the hydrogen bond (H-bond) interactions between the protein and the M1 ligand provide crucial information about the molecular dynamics and stability of this interaction. Several key residues were identified as being involved in hydrogen bonding with the M1 ligand, including Tyr72, Lys156, Ser157, Tyr158, Ser218, and others. These hydrogen bonds are essential for molecular recognition and the formation of a stable bond between protein and ligand, suggesting a critical role for these residues in the specificity of the interaction. At the same time, analysis of the RMSF values highlights the flexibility of certain residues during the interaction with the M1 ligand. Residues including Leu313, Arg315, Tyr316, and Val319 display elevated RMSF values, reflecting substantial mobility in these regions. This flexibility could be associated with conformational changes necessary for the protein to adapt to the presence of ligand. The persistence of this flexibility in residues such as Ser240, Ser241, Asp242 and His 280, independent of the specific ligand (compared to the results with the C3 ligand), suggests a constant structural plasticity in these regions during interactions with different ligands.

These results underline the importance of hydrogen bonds in the molecular recognition between the protein and the M1 ligand, while highlighting the flexibility of certain residues that may play a crucial role in the conformational changes required for the interaction. This information may be valuable for the design of drugs specifically targeting these residues, or for furthering our understanding of the biological mechanisms associated with this protein-ligand interaction.

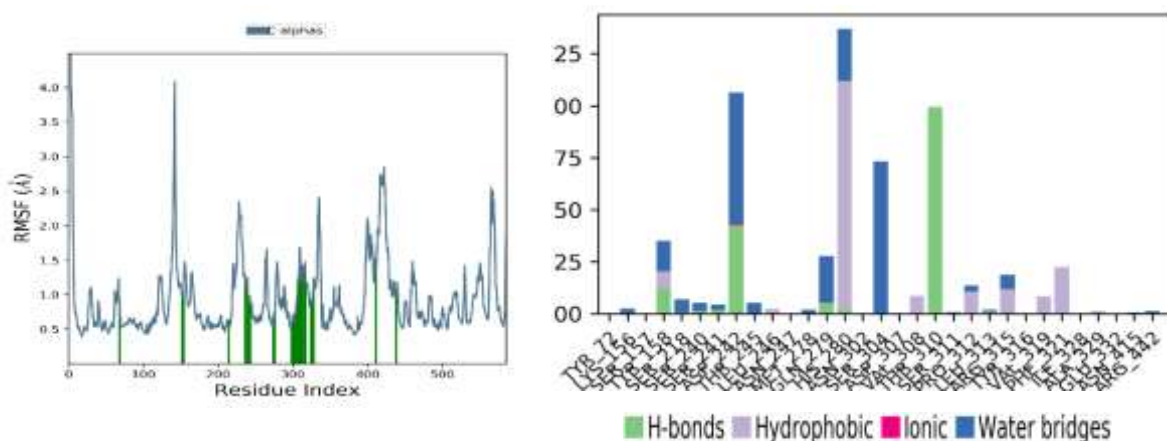


Fig. 12. RMSF of M1 complex amino acids, H-Bonds and fractions of each interaction.

Analysis of the RMSF results and the hydrogen bond (H-bond) interactions between the protein and the M2 ligand provide valuable insight into the molecular dynamics and stability of this particular interaction. Several key residues were identified as being actively involved in hydrogen bonding with the M2 ligand, including Asp69, Lys156, Tyr158, Phe159, and others. These hydrogen bonds play a crucial role in molecular recognition and the formation of a stable bond between protein and ligand, suggesting an important specificity of the interaction.

Analysis of the RMSF values (Fig. 13) also provides information about the flexibility of residues during the interaction with the M2 ligand. Some residues such as Leu313, Pro312, Val319 and others show high RMSF values, indicating significant mobility in these regions. This flexibility could be related to conformational adaptations necessary to accommodate the presence of the ligand. In addition, residues such as Asn414 and Asn415 show particularly high RMSF values, indicating marked flexibility in these regions, which could suggest a functional or structural importance of these residues during interaction with the M2 ligand. These results highlight the specific residues involved in hydrogen bonding with the M2 ligand, underscoring the importance of these interactions for the stability of protein-ligand binding. Furthermore, the flexibility observed in certain residues suggests conformational changes that may be critical for the structural adaptation of the protein upon interaction with the M2 ligand.

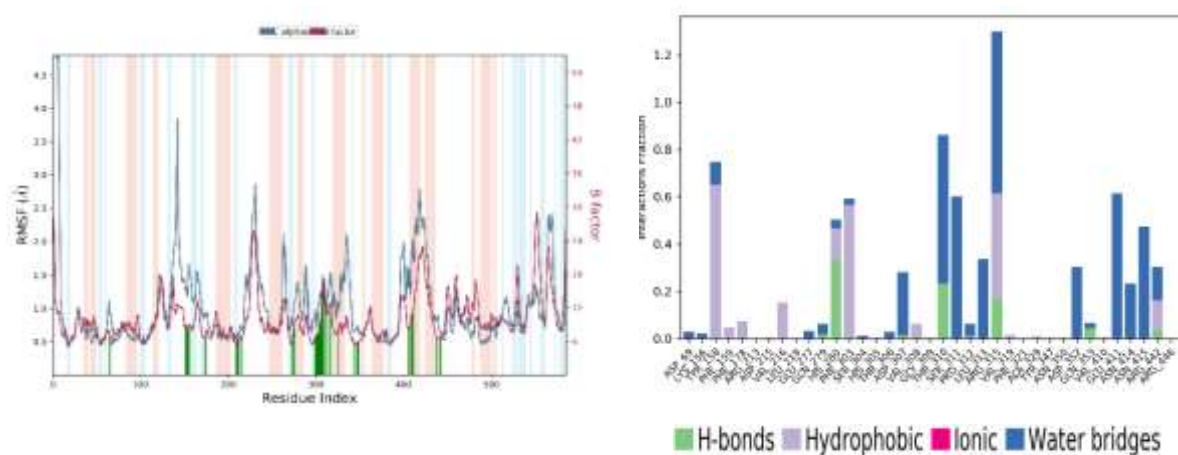


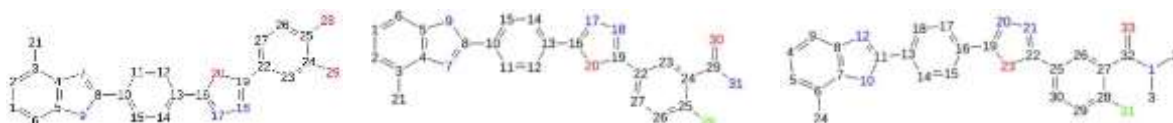
Fig. 13. RMSF of M2 complex amino acids, H-Bonds and fractions of each interaction.

Comparative analysis of the RMSF results for the C3, M1, and M2 ligands reveals significant nuances in the molecular dynamics of each ligand during its interaction with the target protein (Fig. 14). For the C3 ligand, RMSF values relative to the protein indicate a notable flexibility of atoms 21 to 29, suggesting significant fluctuations in these regions during interaction with the protein. RMSF values relative to the ligand itself highlight intrinsically flexible regions of the ligand, suggesting structural adaptability independent of interaction with the protein.

For the M1 ligand, analysis of the RMSF values reveals significant mobility of atoms 21 to 31, with flexibility of atoms 30 and 31, indicating significant conformational changes. Comparison with the C3 ligand highlights different flexibility profiles between the two ligands, underscoring the importance of understanding the specificity of molecular dynamics for each compound.

For the M2 ligand, RMSF analysis highlights pronounced flexibility of atoms 14-18, 24 and 32, suggesting structural adaptability of these regions during the interaction. RMSF values relative to the ligand itself reveal intrinsically flexible zones, with atoms 14 to 18 and 24 to 33 showing significant fluctuations. Comparison with previous ligands highlights specific variations in molecular dynamics between ligands.

These observations underscore the importance of understanding the specific atomic flexibility of each ligand, as it may influence molecular recognition and binding mechanisms with the target protein. Such detailed understanding can guide drug design by identifying flexible regions as potential targets for optimization of ligand-protein interaction. The RMSF analysis shown in Fig. 14 provides in-depth insight into the molecular dynamics of each ligand, opening prospects for the development of more effective M1 and M2 compounds based on their distinct flexibility profiles.



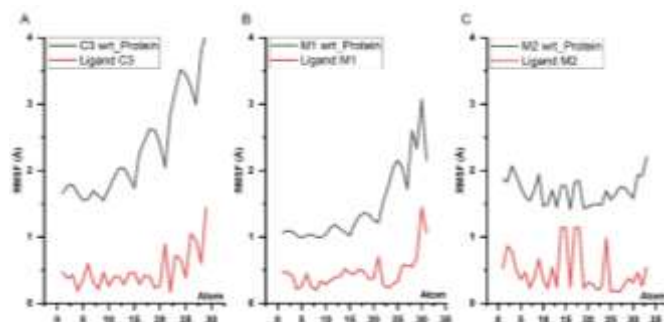


Fig. 14. RMSF of the more active C3 molecule (A) and the candidate compounds M1 (B) and M2 (C).

Studying the interactions between the C3 ligand and the target amino acids during molecular dynamics simulations provides valuable insights into potential binding sites. First, the C3 ligand showed a significant affinity for the amino acid Thr310, establishing contacts within the first 125 nanoseconds and between 140 and 200 nanoseconds. This bifurcated interaction suggests a temporal dynamic in the binding of the C3 ligand to Thr310.

Similar interactions were observed with other amino acids. Between 85 and 200 nanoseconds, the C3 ligand is in contact with Asp307, highlighting a later, more prolonged interaction. An early interaction was observed with His280, lasting from 0 to 48 nanoseconds, indicating initial binding early in the simulation. Contact with Phe303 was established from 80 to 200 nanoseconds, demonstrating a prolonged interaction.

These residues were identified as forming a maximum of three bonds with the C3 ligand, suggesting specificity in preferred binding sites. However, with other amino acids, the C3 ligand formed bonds discontinuously, highlighting the diversity of possible interactions.

Overall, the C3 ligand showed a variable number of contacts, oscillating between 4 and 12. This variability may reflect the plasticity of the C3 ligand in its interactions with different sites on the target protein, underscoring the complexity of the molecular mechanisms involved.

In parallel with the interaction analysis, protein secondary structure elements (SSEs) were monitored throughout the simulation. The results show a significant distribution of helices (25.11%), alpha structures (13.54%) and beta chains (34.67%). Fig. 15 illustrates the distribution of these SSEs by residue index in the protein structure, providing further information on the structural dynamics of the protein during the simulation.

In summary, this detailed analysis of the specific interactions of the C3 ligand with the target amino acids, coupled with the monitoring of SSEs, provides an in-depth understanding of the molecular mechanisms involved, facilitating the evaluation of the potential performance of the C3 ligand as a drug candidate.

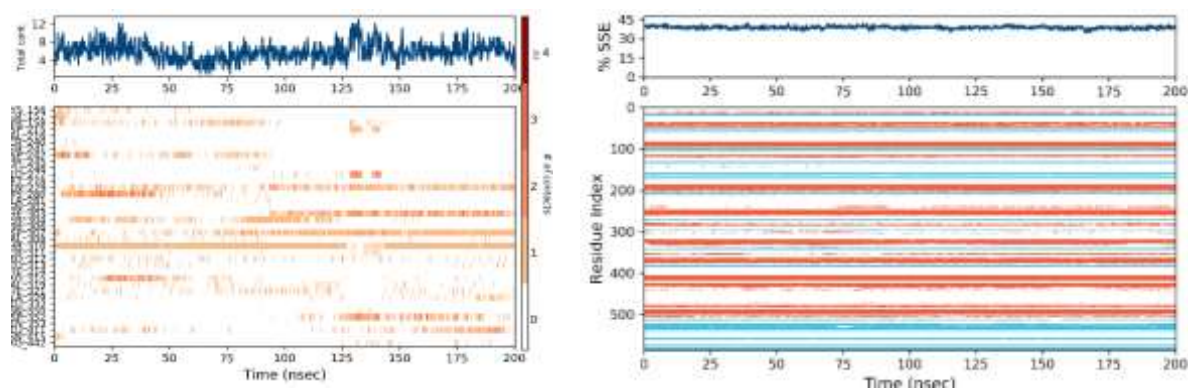


Fig. 15. Total number of interactions between the C3 ligands and the tracking of ligand-protein contacts with a weight of 200 ns.

Analysis of the interactions between the ligand M1 and the target amino acids during the molecular dynamics simulation provides detailed insight into the nature of the bonds formed and the stability of these interactions.

First, the M1 ligand showed a consistent interaction with the Thr310 amino acid throughout the simulation. This persistent binding suggests a significant affinity between the M1 ligand and Thr 310, indicating a potentially critical binding site for the biological activity of the ligand (Fig. 16).

The M1 ligand intermittently formed bonds with the amino acid SER 304. The intermittent nature of these bonds may reflect a sensitivity of the M1 ligand to the dynamics of the target protein at this specific site.

On the other hand, the M1 ligand maintained almost constant contact with amino acids His 280 and Asp 242 throughout the simulation. The variability in the number of bonds, ranging from two to three, suggests some plasticity in these interactions and underscores the complexity of the molecular relationships between the M1 ligand and these residues.

The interaction of the M1 ligand with the Tyr158 amino acid was characterized by constant contact and sometimes the formation of more than one chemical bond. This suggests a dynamic interaction with variations in the number of bonds, which could be related to the flexibility of the binding region.

Finally, the total number of contacts between the M1 ligand and the target amino acids ranged from 3 to 9 bonds. This wide range demonstrates the ability of the M1 ligand to interact with different binding sites within the target protein, with the M1 ligand showing remarkable interaction specificity with certain amino acids, maintaining constant bonds with Thr310, Tyr158, and intermittent interactions with Ser304. The variety in the number of bonds with His 280 and Asp 242 suggests flexibility in these interactions. These results provide critical information on the mechanisms by which the M1 ligand interacts with its target, which may be essential for its potential as a drug candidate.

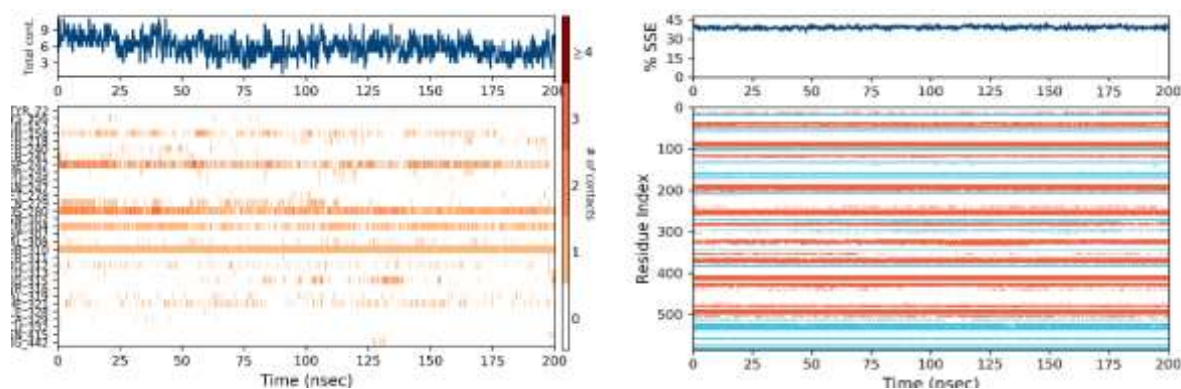


Fig. 16. Total number of interactions between the M1 ligands and the tracking of ligand-protein contacts with a weight of 200 ns.

Analysis of the contact tracking between the M2 ligand and the target amino acids during the 200 nanosecond molecular dynamics simulation reveals complex and varied dynamic interactions.

First, the M2 ligand showed a particular affinity for the amino acid Tyr158, discretely forming more than two bonds throughout the simulation. This persistent interaction suggests a strong affinity between the M2 ligand and Tyr158, which may have important implications for molecular recognition (Fig. 17).

Interestingly, the M2 ligand also showed dynamics in its interactions with other amino acids. Between 30 and 85 nanoseconds, the M2 ligand sometimes formed three bonds with the amino acid His280, highlighting the plasticity of molecular interactions over time.

In addition, the M2 ligand temporarily formed two bonds with the Phe303 amino acid from the beginning of the simulation to 120 nanoseconds. This variation in the number of bonds may reflect the adaptability of the M2 ligand in its interactions with different residues.

A notable interaction was observed with the amino acid Thr310, with the continuous formation of a single bond throughout the simulation. This suggests a constant and specific interaction between the M2 ligand and Thr310.

Between 58 and 182 nanoseconds, the M2 ligand formed a bond with the Ser311 amino acid, indicating a new dynamic interaction at another potential binding site.

During the first 50 nanoseconds, more than three bonds were formed between the M2 ligand and the amino acid Arg315. Thereafter, the M2 ligand remained in contact, discretely forming between 1 and 3 bonds. This variability in the number of bonds highlights the complexity of the interactions between the M2 ligand and Arg315.

Overall, the M2 ligand showed a diversity of interactions with different target amino acids, reflecting structural adaptability. The total number of contacts, which varied between 4 and 12, suggests a dynamic performance of this engineered molecule, opening up promising prospects for its potential as a pharmaceutical ligand. These detailed results provide critical information for understanding the molecular interaction mechanisms of the M2 ligand with its target.

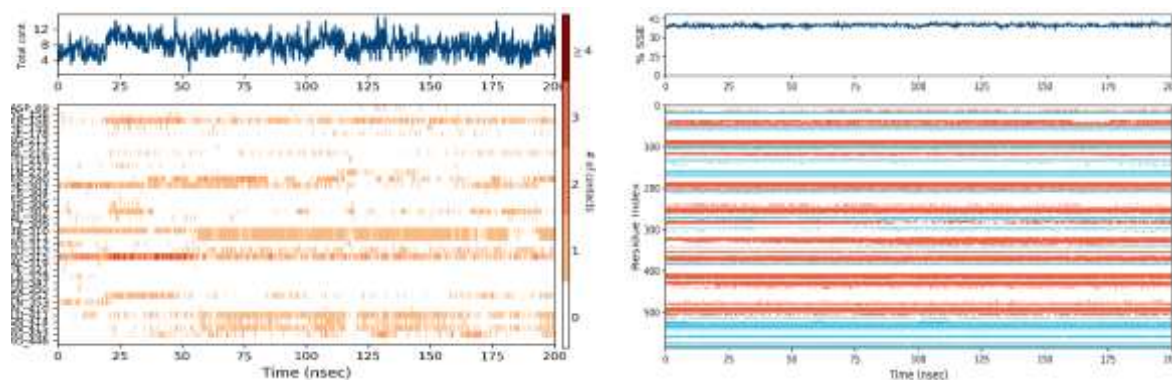


Figure 17. Total number of interactions between the M2 ligands and the tracking of ligand-protein contacts with a weight of 200 ns.

Analysis of the results of molecular dynamics simulations of the C3, M1 and M2 ligands over a period of 200 nanoseconds reveals significant differences in their structural and dynamic properties. In terms of radius of gyration (rGyr), the C3 ligand shows significantly higher compactness compared to M1 and M2, indicating a denser structure (Fig. 18A). Variations over time also suggest greater potential structural stability for the C3 ligand. In terms of molecular surface area (MolSA), the M2 ligand stands out as having the largest surface area, closely followed by M1, while C3 has the smallest molecular surface area (Fig. 18B). This observation suggests significant differences in molecular size between the ligands. Furthermore, accessible surface area (SASA) analysis indicates that the M2 ligand generally exhibits greater accessibility to its environment, which may have implications for its interactions with other molecules (Fig. 18C). Finally, polarizable surface area (PSA) reveals notable differences in polar interaction properties, with the M2 ligand exhibiting a smaller polarizable surface area compared to C3 and M1 (Fig. 18D). These results highlight the importance of understanding the molecular differences between C3, M1 and M2 ligands, which may have significant implications in specific biological or pharmacological contexts.

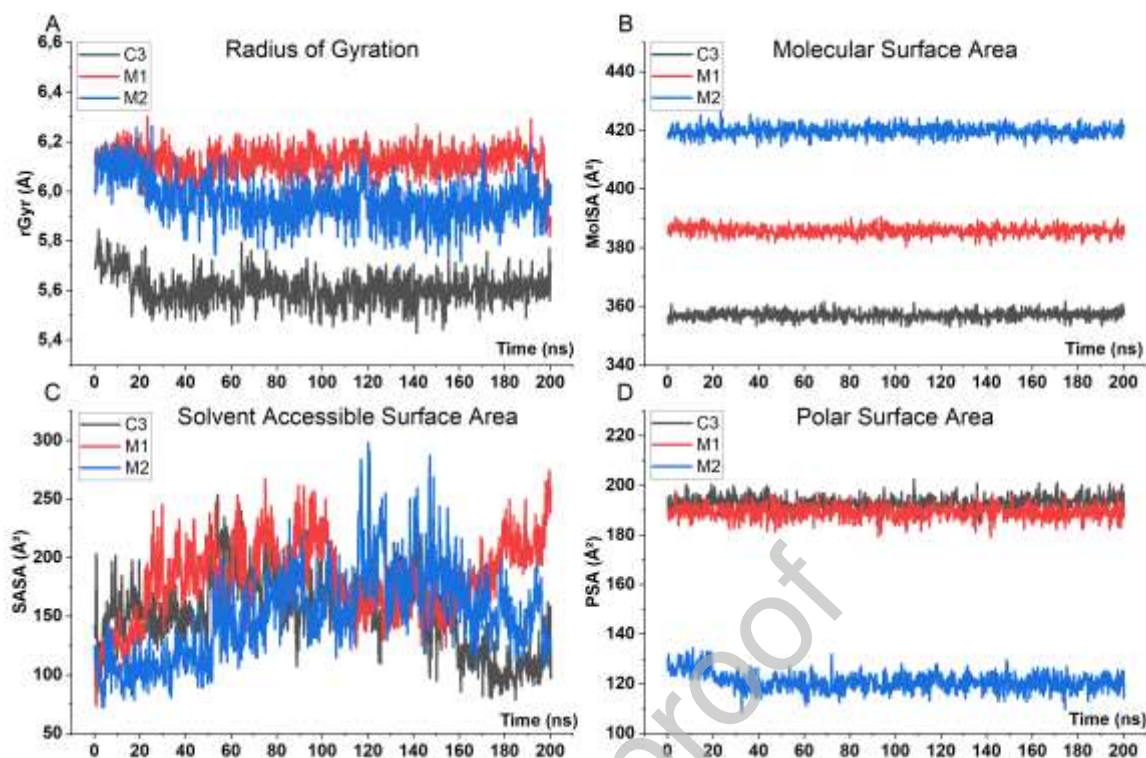


Fig. 18. Molecular descriptors in the analysis of ligands C3, M1, and M2.

DFT Result

Conceptual Density Functional Theory (CDFT) known as the reactivity analysis based branch of Density Functional Theory (DFT) presents simple and useful equations and electronic structure principles and equations about reactivity analysis descriptors such as chemical potential (μ), electronegativity (χ), hardness (η) and softness (σ). The mathematical relations for the computation of these descriptors are given as [72,77,78]:

$$\chi = -\mu = -\left[\frac{\partial E}{\partial N}\right]_{v(r)} = \frac{I + A}{2} \quad (8)$$

$$\eta = \left[\frac{\partial \mu}{\partial N}\right]_{v(r)} = \left[\frac{\partial^2 E}{\partial N^2}\right]_{v(r)} = I - A \quad (9)$$

$$\sigma = 1/\eta \quad (10)$$

In the given mathematical relations, E, N, I and A are total electronic energy, total number of the electrons, ground state ionization energy and ground state electron affinity of the studied chemical system, respectively. To predict the ionization energy and electron affinity of the C3, M1 and M2

molecules, we used the Koopmans Theorem giving the following orbital energy based formulae [79].

$$I = -E_{HOMO} \quad (11)$$

$$A = -E_{LUMO} \quad (12)$$

where, E_{HOMO} and E_{LUMO} are the energies of HOMO and LUMO orbitals, respectively.

Parr, Szentpaly and Liu introduced the electrophilicity index (ω) as the square of the electronegativity divided by twice the hardness [80].

$$\omega = \chi^2 / 2\eta \quad (13)$$

The electronic structure principles such as Maximum Hardness, Minimum Polarizability and Minimum Electrophilicity Principles present the relationship of the corresponding property to chemical reactivity. Chemical hardness introduced by Pearson via Hard and Soft Acid-Base (HSAB) Principle classifying the Lewis acid-bases as hard, soft and borderline is reported as the resistance against polarization of atomic and molecular chemical systems [71-83].

The relation with stability of the chemical hardness is given via Maximum Hardness Principle (MHP). According to MHP, "there seems to be a rule of nature that molecules arrange themselves so as to be as hard as possible." This statement implies that chemical hardness is a reliable measure of stability. Hard chemical systems that resist polarization exhibit high stability [84-86].

The electronic structure principle showing the relation between reactivity and electrophilicity index is Minimum Electrophilicity Principle proposed by Chamorro and coworkers [86].

In proposing this principle, the authors argued that electrophilicity is minimized at stable states. Both Maximum Hardness and Minimum Electrophilicity Principles imply that the most stable chemical system among the selected compounds in Table 13 is C3 while the most reactive one is M1.

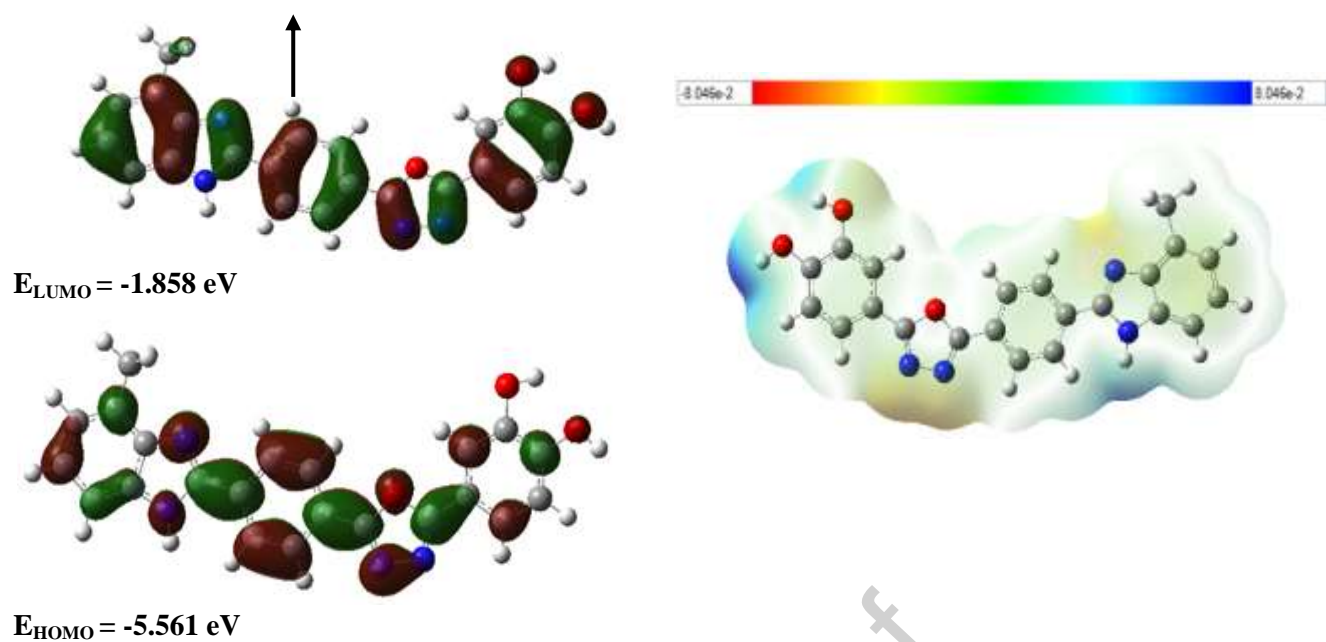


Fig. 19. HOMO-LUMO representation, and ESP representation of the compound C3

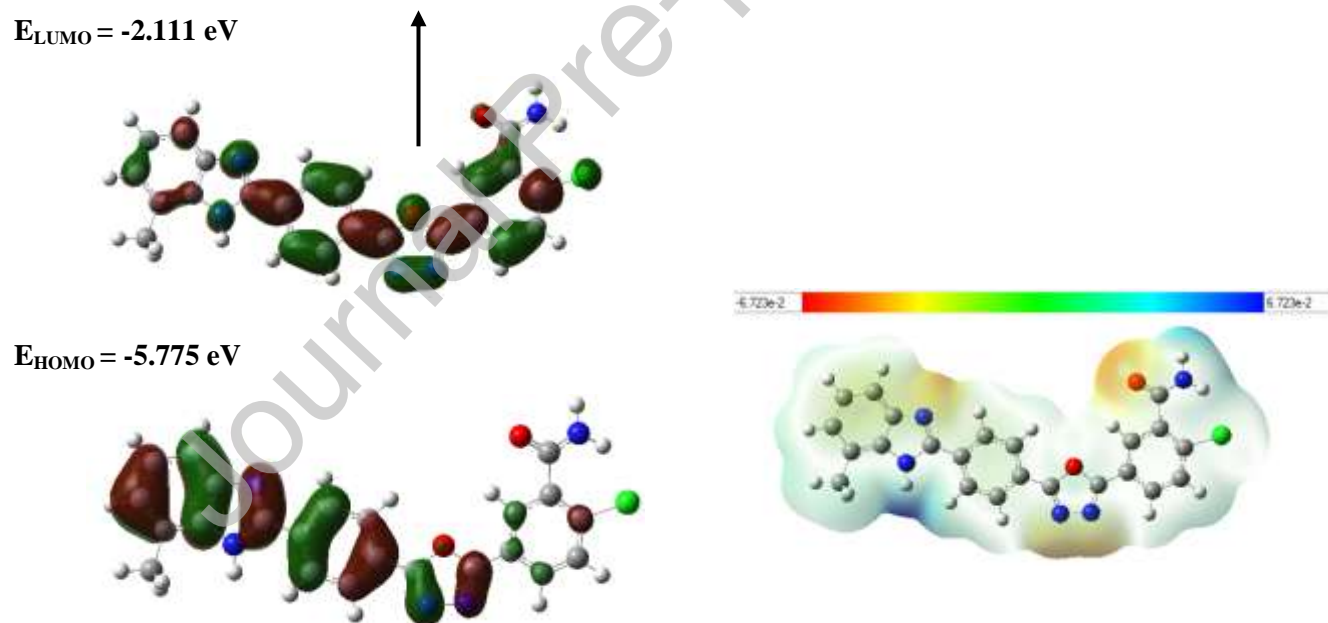


Fig. 20. HOMO-LUMO representation, and ESP representation of the compound M1

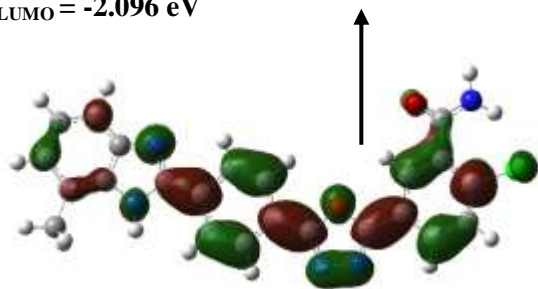
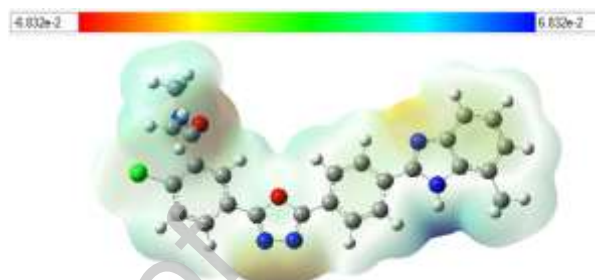
$E_{\text{LUMO}} = -2.096 \text{ eV}$  $E_{\text{HOMO}} = -5.797 \text{ eV}$ 

Fig. 21. HOMO-LUMO representation, and ESP representation of the compound M2

Table 13. Reactivity indices of the selected compounds

Parameter/compound	C3	M1	M2
E_{HOMO}	-5.561	-5.775	-5.797
E_{LUMO}	-1.858	-2.111	-2.096
Ionization potential	5.561	5.775	5.797
Electron affinity	1.858	2.111	2.096
Energy gap (ΔE)	3.703	3.664	3.701
Electronegativity χ	3.709	3.943	3.946
Chemical potential μ	-3.709	-3.943	-3.946
Chemical hardness η	3.703	3.664	3.701
Global softness σ	0.270	0.273	0.270
Electrophilicity index ω	1.858	2.122	2.104
Nucleophilicity index N	3.807	3.593	3.571

Conclusion

In this paper, a set of 20 benzimidazole-based oxadiazole molecules was investigated using 3D-QSAR approach. The CoMFA and CoMSIA/SED models demonstrated important statistical quality and excellent predictive competency. The recommended models were employed to produce the contour maps that help to identify the main regions impacting the α -glucosidase activity. Thus, four new potent benzimidazole-based oxadiazole molecules were proposed with important inhibitory activity. ADME/Tox results demonstrated that the new candidate molecules possess excellent pharmacokinetic properties and bioavailability, comply with drug-likeness

criteria, and have high synthetic accessibility, making them both effective and easy to synthesize. Furthermore, molecular docking findings provide adequate details to comprehend the binding mode of the benzimidazole-based oxadiazole inhibitors with the target receptor. The new proposed molecules M1 and M2 demonstrated strong interactions, displaying favorable binding characteristics. MD simulation showed good stability of the compounds M1 and M2 during the 200 ns. The reactivity and stability of the compounds were discussed in the light of the popular electronic structure principles. Both maximum hardness and minimum electrophilicity principles supported the high stability of compound C3. In the next work, we will carry out the activity test, including enzyme activity, cytotoxicity, and *in vivo* hypoglycemic effects of the compound M1 which is demonstrated promising *in silico* result.

Acknowledgments

We dedicate this work to the “Moroccan Association of Theoretical Chemists” (MATC) for its pertinent help concerning the programs.

References

- [1] A. Khaldan, S. Bouamrane, R. El-mernissi, M. Ouabane, M. Alaqarbeh, H. Maghat, M.A. Ajana, C. Sekkat, M. Bouachrine, T. Lakhliifi, A. Sbai, Design of new α -glucosidase inhibitors through a combination of 3D-QSAR, ADMET screening, molecular docking, molecular dynamics simulations and quantum studies. *Arab. J. Chem.* 17 (2024) 105656.
- [2] S. Hayat, H. Ullah, F. Rahim, I. Ullah, M. Taha, N. Iqbal, F. Khan, M.S. Khan, S.A.A. Shah, A. Wadood, M. Sajid, A.N. Abdalla, Synthesis, biological evaluation and molecular docking study of benzimidazole derivatives as α -glucosidase inhibitors and anti-diabetes candidates, *J. Mol. Struct.* 1276 (2023) 134774.
- [3] C. Hu, B. Liang, J. Sun, J. Li, Z. Xiong, S.H. Wang, X. Xuetao, Synthesis and biological evaluation of indole derivatives containing thiazolidine-2,4-dione as α -glucosidase inhibitors with antidiabetic activity, *Eur J Med Chem*, 264 (2024) 115957.
- [4] D. Tomic, J.E. Shaw, D.J. Magliano, The burden and risks of emerging complications of diabetes mellitus, *Nat Rev Endocrinol.* 18 (2022) 525-539.
- [5] M. Taha, A.A. Khan, F. Rahim, S. Hayat, S. Imran, N. Iqbal, N. Uddin, K.M. Khan, E.H. Anouar, R.K. Farooq, M. Nawaz, S.A.A. Shah, Synthesis, *in vitro* evaluation and molecular docking studies of hybrid 4-quinoliny bearing 1,3,4-thiadiazole-2-amine as a new inhibitor of α -amylase and α -glucosidase, *J. Mol. Struct.* 1282 (2023) 135173.
- [6] D.R. Whiting, L. Guariguata, C. Weil, J. Shaw, IDF diabetes atlas: global estimates of the prevalence of diabetes for 2011 and 2030. *Diabetes Research and Clinical Practice*, 94 (2011) 311–321.
- [7] M. Taha, F. Rahim, K. Zaman, M. Selvaraj, N. Uddin, R.K. Farooq, M. Nawaz, M. Sajid, F. Nawaz, M. Ibrahim, K.M. Khan, Synthesis, α -glycosidase inhibitory potential and molecular docking study of benzimidazole derivatives. *Bioorganic Chemistry*, 95 (2020) 103555.
- [8] F. Rahim, H. Ullah, R. Hussain, M. Taha, S. Khan, M. Nawaz, F. Nawaz, S. J. Gilani, M. N. B. Jumah, Thiadiazole based triazole/hydrazone derivatives: Synthesis, *in vitro* α -glucosidase inhibitory activity and *in silico* molecular docking study, *J. Mol. Struct.* 1287 (2023) 135619.

- [9] A. Khaldan, K. El khatabi, R.El-Mernissi, A. Ghaleb, R. Hmamouchi, A. Sbai, M. Bouachrine, T. Lakhli, 3D-QSAR Modeling and Molecular Docking Studies of novel triazoles-quinine derivatives as antimalarial agents. *Journal of Materials and Environmental Sciences*, 11 (2020) 429-443.
- [10] R. Hussain, W. Rehman, F. Rahim, S. Khan, M. Taha, Y. Khan, A. Sardar, I. Khan, S.A.A. Shah, Discovery of imidazopyridine derived oxadiazole-based thiourea derivatives as potential anti-diabetic agents: Synthesis, in vitro antioxidant screening and in silico molecular modeling approaches, *J. Mol. Struc.* 1293 (2023) 136185.
- [11] A. Khaldan, S. Bouamrane, R. El-mernissi, H. Maghat, M.A. Ajana, A. Sbai, M. Bouachrine, T. Lakhli, Identification of potential α -glucosidase inhibitors: 3D-QSAR modeling, molecular docking approach, *Rhazes: Green and applied chemistry*, 12 (2021) 60-7.
- [12] G.J. Ye, T. Lan, Z.X. Huang, X.N. Cheng, C.Y. Cai, S.M. Ding, M.L. Xie, B. Wang, Design and synthesis of novel xanthone-triazole derivatives as potential antidiabetic agents: α -Glucosidase inhibition and glucose uptake promotion, *Eur J Med Chem.* 177 (2019) 362-373.
- [13] M. Li, J. Sun, B. Liang, X. Min, J. Hu, R. Wu, X. Xu, Thiazolidine-2,4-dione derivatives as potential α -glucosidase inhibitors: Synthesis, inhibitory activity, binding interaction and hypoglycemic activity, *Bioorg Chem*, 144 (2024) 107177.
- [14] B. Liang, D. Xiao, S.H. Wang, X. Xu, Novel thiosemicarbazide-based β -carboline derivatives as α -glucosidase inhibitors: Synthesis and biological evaluation, *Eur J Med Chem* 275 (2024) 116595
- [15] M. Taha, S. Hayat, F. Rahim, N. Uddin, A. Wadood, M. Nawaz, M. Gollapalli, A. Ur Rehman, K.M. Khan, R.K. Farooq, Exploring thiazole-based Schiff base analogs as potent α -glucosidase and α -amylase inhibitor: their synthesis and in-silico study, *J. Mol. Struc.* 1287 (2023) 135672.
- [16] M. Taha, F.J. Alshamrani, F. Rahim, S. Hayat, H. Ullah, K. Zaman, S. Imran, K.M. Khan, F. Naz, Synthesis of Novel Triazinoindole-Based Thiourea Hybrid: A Study on α -Glucosidase Inhibitors and Their Molecular Docking, *Molecules*, 24 (2019) 3819.
- [17] A. Khaldan, S. Bouamrane, R. El-Mernissi, M. Alaqarbeh, H. Maghat, M. Bouachrine, T. Lakhli, A. Sbai, Integrated Computer Aided Methods to Designing Potent α -Glucosidase Inhibitors Based on Quinoline Scaffold Derivatives, *Curr. Chem. Lett.* 14 (2025) 79–106.
- [18] A. Khaldan, S. Bouamrane, R. El-mernissi, L. El Mchichi, H. Maghat, M.A. Ajana, A. Sbai, M. Bouachrine, T. Lakhli, In search of new potent α -glucosidase inhibitors: molecular docking and ADMET prediction, *Mor. J. Chem.* 10 (2022) 772-786.
- [19] X-Z. Wu, W-J. Zhu, L. Lu, C-M. Hu, Y-Y. Zheng, X. Zhang, J. Lin, J-Y. Wu, Z. Xiong, K. Zhang, X-T. Xu, Synthesis and anti- α -glucosidase activity evaluation of betulinic acid derivatives, *Arabian Journal of Chemistry*, 16 (2023) 104659.
- [20] H. Ullah, F. Rahim, M. Taha, R. Hussain, N. Tabassum, A. Wadood, M. Nawaz, A. Mosaddik, S. Imran, Z. Wahab, G. Abbas Miana, Kanwal, K. Mohammed Khan, Aryl-oxadiazole Schiff bases: Synthesis, α -glucosidase in vitro inhibitory activity and their in silico studies, *Arab. J. Chem*, 13 (2020) 4904-4915.
- [21] J.L. Chiasson, R.G. Josse, R. Gomis, M. Hanefeld, A. Karasik, M. Laakso, Acarbose Treatment and the Risk of Cardiovascular Disease and Hypertension in Patients With Impaired Glucose Tolerance, *J. Am. Med. Assoc.* 290 (2003) 486-494.
- [22] A. Khaldan, S. Bouamrane, R. El-Mernissi, K. El Khatabi, I. Aanouz, A. Aggoram, A. Sbai, M. Bouachrine, T. Lakhli, QSAR study of α -Glucosidase inhibitors for benzimidazole bearing bis-Schiff bases using CoMFA, CoMSIA, and molecular docking, *International Journal of Quantitative Structure-Property Relationships*, 6 (2021) 9–24.

- [23] M. Saeedi, M. Mohammadi-Khanaposhtani, M.S. Sgari, N. Eghbalnejad, S. Imanparast, M.A. Faramarzi, B. Larijani, M. Mahdavi, T. Akbarzadeh, Design, synthesis, in vitro, and in silico studies of novel diarylimidazole-1,2,3-triazole hybrids as potent α -glucosidase inhibitors, *Bioorg Med Chem.* 27(2019) 115148.
- [24] H. Ullah, S. Khan, F. Rahim, M. Taha, R. Iqbal, M. Sarfraz, S.A.A. Shah, M. Sajid, M.F. Awad, A. Omran, M.A. Albalawi, M.A. Abdelaziz, A. Al Areefy, I. Jafri, Benzimidazole Bearing Thiosemicarbazone Derivatives Act as Potent α -Amylase and α -Glucosidase Inhibitors; Synthesis, Bioactivity Screening and Molecular Docking Study, *Molecules*, 27 (2022) 6921.
- [25] H. Azizian, K. Pedrood, A. Moazzam, Y. Valizadeh, K. Khavaninzadeh, A. Zamani, M. Mohammadi-Khanaposhtani, S. Mojtavavi, M.A. Faramarzi, S. Hosseini, Y. Sarrafi, H. Adibi, B. Larijani, H. Rastegar, M. Mahdavi, Docking study, molecular dynamic, synthesis, anti- α -glucosidase assessment, and ADMET prediction of new benzimidazole-Schiff base derivatives, *Sci Rep*, 12 (2022) 14870.
- [26] R. Kawamori, N. Tajima, Y. Iwamoto, A. Kashiwagi, K. Shimamoto, K. Kaku, Voglibose for prevention of type 2 diabetes mellitus: a randomised, double-blind trial in Japanese individuals with impaired glucose tolerance, *Lancet.* 373 (2009) 1607-1614.
- [27] S. Tahlan, S. Kumar, B. Narasimhan, Pharmacological significance of heterocyclic 1 H-benzimidazole scaffolds: a review, *BMC. Chem*, 13 (2019) 101.
- [28] K. Shah, S. Chhabra, S.K. Shrivastava, P. Mishra, Benzimidazole: A promising pharmacophore, *Med. Chem. Res.* 22 (2013) 5077–5104.
- [29] M.S. Vasava, M.N. Bhoi, S.K. Rathwa, D.J. Jethava, P.T. Acharya, D.B. Patel, H.D. Patel, Benzimidazole: A Milestone in the Field of Medicinal Chemistry, *Mini. Rev. Med. Chem*, 20 (2020) 532–565.
- [30] Y. Bansal, O. Silakari, The therapeutic journey of benzimidazoles: a review, *Bioorg. Med. Chem*, 20 (2012) 6208–6236.
- [31] G. Singh, M. Kaur, M. Chander, The latest information on biological activities, *Int. Res. J. Pharm.* 1 (2013) 82–87.
- [32] R.V. Shingalapur, K.M. Hosamani, R.S. Keri, M.H. Hugar, Derivatives of benzimidazole pharmacophore: synthesis, anticonvulsant, antidiabetic and DNA cleavage studies, *Eur. J. Med. Chem.* 45 (2010) 1753-1759.
- [33] Y. Luo, J.P. Yao, L. Yang, C. L. Feng, W. Tang, G.F. Wang, W. Lu, Design and synthesis of novel benzimidazole derivatives as inhibitors of hepatitis B virus, *Bioorg. Med. Chem.* 18 (2010) 5048-5055.
- [34] K. Achar, K.M. Hosamani, H.R. Seetharamareddy, In-vivo analgesic and anti-inflammatory activities of newly synthesized benzimidazole derivatives, *Eur. J. Med.Chem.* 45 (2010) 2048-2054.
- [35] Z. S.Saify, A. Kamil, S. Akhtar, M. Taha, A. Khan, K. M. Khan, S. Jahan, F. Rahim, S. Perveen, M. I. Choudhary, 2-(2'-Pyridyl) benzimidazole derivatives and their urease inhibitory activity, *Med. Chem. Res.* 23 (2014) 4447-4454.
- [36] V. Padmavathi, B.C. Venkatesh, A. Muralikrishna, A. Padmaja, The reactivity of gem cyanoester ketene dithiolates towards the development of potent antioxidant heterocycles, *Chem. Pharm. Bull.* 60 (2012), 449-4458.
- [37] M. Ishikawa, K. Nonoshita, Y. Ogino, Y. Nagae, D. Tsukahara, H. Hosaka, H. Hosaka, H. Maruki, S. Ohyama, R. Yoshimoto, K. Sasaki, Y. Nagata, T. Nishimura, Discovery of novel 2-(pyridine-2-yl)-1H-benzimidazole derivatives as potent glucokinase activators, *Bioorg. Med. Chem. Lett.* 19 (2009) 4450-4454.
- [38] J. Boström, A. Hogner, A. Llinàs, E. Wellner, A.T. Plowright, Oxadiazoles in medicinal chemistry, *J. Med. Chem.* 55 (2012) 1817–1830.

- [39] M.A. Zhang, N. Mulholland, D.T. Beattie, D. Irwin, Y. Gu, Q. Chen, et al., Synthesis and antifungal activity of 3-(1,3,4-oxadiazol-5-yl)-indoles and 3-(1,3,4-oxadiazol-5-yl) methyl-indoles, *Eur. J. Med. Chem.* 63 (2013) 22–32.
- [40] A. Khaldan, S. Bouamrane, R. El-mernissi, H. Maghat, A. Sbai, M. Bouachrine, T. Lakhliifi, Molecular docking, ADMET prediction, and quantum computational on 2-methoxy benzoyl hydrazone compounds as potential antileishmanial inhibitors, *Biointerface Research in Applied Chemistry*. 4 (2023), 302.
- [41] K. El Khatabi, I. Aanouz, R. EL-Mernissi, A. Khaldan, M.A. Ajana, M. Bouachrine, T. Lakhliifi, Design of Novel Benzimidazole Derivatives as Potential α -amylase Inhibitors by 3D-QSAR Modeling and Molecular Docking Studies, *Journal of the Turkish Chemical Society Section A: Chemistry*. 7 (2020) 471-480.
- [42] R. EL-Mernissi, A. Khaldan, S. Bouamrane, H.M. Rehman, M. Alaqarbeh, M.A. Ajana, T. Lakhliifi, M. Bouachrine, 3D-QSAR, molecular docking, simulation dynamic and ADMET studies on new quinolines derivatives against colorectal carcinoma activity, *J. Biomol. Struct. Dyn.* 42 (2024) 3682-3699.
- [43] S. Bouamrane, A. Khaldan, H. Maghat, M.A. Ajana, M. Bouachrine, T. Lakhliifi, in-silico design of new triazole analogs using QSAR and molecular docking models, *Rhazes: Green and Applied Chemistry*, 11 (2021) 223- 236.
- [44] A. Khaldan, A. Agorram, A. Ghaleb, A. Aouidate, A. Sbai, M. Bouachrine, T. Lakhliifi, 3D QSAR Modeling and Molecular Docking Studies on a series of quinolone-triazole derivatives as antibacterial agents, *Rhazes: Green and Applied Chemistry*, 6 (2019) 11-26.
- [45] R. EL-Mernissi, K. El Khatabi, A. Khaldan, L. El Mchichi, M.A. Ajana, M. Bouachrine, T. Lakhliifi, 3D-QSAR, ADMET, and molecular docking studies for designing New 1,3,5-triazine derivatives as anticancer agents, *Egypt. J. Chem.* 65 (2022) 9 - 18
- [46] G. Klebe, U. Abraham, T. Mietzner, Molecular similarity indices in a comparative analysis (CoMSIA) of drug molecules to correlate and predict their biological activity, *J. Med. Chem.* 37 (1994) 4130–4146.
- [47] R.D. Cramer, D.E. Patterson, J.D. Bunce, Comparative molecular field analysis (CoMFA). 1. Effect of shape on binding of steroids to carrier proteins, *J. Am. Chem. Soc.* 110 (1988) 5959–5967.
- [48] R. EL-Mernissi, K. El Khatabi, A. Khaldan, S. Bouamrane, L. El Mchichi, M.A. Ajana, M. Bouachrine, T. Lakhliifi, Designing of novel quinolines derivatives as hepatocellular carcinoma inhibitors by using in silico approaches, *Biointerface. Res. Appl. Chem*, 13 (2023) 217.
- [49] A. Khaldan, S. Bouamrane, R. El-mernissi, H. Maghat, A. Sbai, M. Bouachrine, T. Lakhliifi, molecular docking, ADMET prediction and quantum computational on 2-methoxy benzoyl hydrazone compounds as potential antileishmanial inhibitors, *Biointerface. Res. Appl. Chem.* 4 (2023) 302.
- [50] S. Bouamrane, A. Khaldan, M. Alaqarbeh, A. Sbai, M.A. Ajana, M. Bouachrine, T. Lakhliifi, H. Maghat, Computational integration for antifungal 1,2,4-triazole inhibitors design: QSAR, molecular docking, molecular dynamics simulations, ADME/Tox, and retrosynthesis studies, *Chemical Physics Impact*, 8 (2024) 100502.
- [51] S. Bouamrane, A. Khaldan, M. Alaqarbeh, A. Sbai, M.A. Ajana, M. Bouachrine, T. Lakhliifi, H. Maghat, Garlic as an effective antifungal inhibitor: A combination of reverse docking, molecular dynamics simulation, ADMET screening, DFT, and retrosynthesis studies, *Arab. Chem. J.* 17 (2024) 105642.
- [52] A. Khaldan, S. Bouamrane, A. Aouidate, H. Maghat, A. Sbai, M. Bouachrine, T. Lakhliifi, 3D-QSAR study of urease inhibitors for arylhydrazide Schiff bases derivative s via CoMFA, CoMSIA and molecular docking, *Rhazes: Green and Applied Chemistry*, 11 (2021) 238-251.

- [53] S. Bouamrane, A. Khaldan, H. Maghat, M.A. Ajana, M. Bouachrine, T. Lakhlifi, Quantitative Structure-Activity Relationships and Molecular Docking studies of 1.2.4 triazole derivatives as antifungal activity, *Rhazes: Green and Applied Chemistry*, 10 (2020) 33-48.
- [54] R. El-Mernissi, K. El Khatabi, A. Khaldan, S. Bouamrane, M.A. Ajana, T. Lakhlifi, M. Bouachrine, New compounds based on 1H-pyrrolo [2, 3-b] pyridine as potent TNIK inhibitors against colorectal cancer cells. Molecular modeling studies, *Mor. J. Chem.* 11 (2023) 20-33
- [55] A. Belhassan, S. Chtita, H. Zaki, M. Alaqarbeh, N. Alsakhen, F. Almohtaseb, T. Lakhlifi, M. Bouachrine, In silico detection of potential inhibitors from vitamins and their derivatives compounds against SARS-CoV-2 main protease by using molecular docking, molecular dynamic simulation and ADMET profiling, *J Mol Struct.* 1258 (2022) 132652
- [56] S. Srivastava, S. Pandey, A. Kumar, S. A. Siddiqui, K. D. Dubey, Synthesis ADMET molecular docking, MD simulation and MM-PBSA investigations of a novel hetero-steroid with Anti-proliferative and Anti-inflammatory properties, *J. Mol. Struct.* 1321 (2025) 139783.
- [57] Sybyl 8.1; Tripos Inc.: St. Louis, MO, USA, 2008; Available online: <http://www.tripos.com> (accessed on 26 January 2011).
- [58] M. Clark, R.D. Cramer, N. Van Opdenbosch, Validation of the general purpose tripos 5.2 force field, *J. Comput. Chem.* 10 (1989) 982–1012.
- [59] S. Wold, Validation of QSAR's. Quantitative Structure Activity Relationships, 10 (1991) 191–193.
- [60] A. Golbraikh, A. Tropsha, Beware of q^2 !. *J. Mol. Graph. Model.* 20 (2002) 269–276.
- [61] K. Roy, On some aspects of validation of predictive quantitative structure–activity relationship models, *Expert. Opin. Drug. Discov.* 2 (2007) 1567–1577.
- [62] C. Rücker, G. Rücker, M. Meringer, γ -Randomization and Its Variants in QSPR/QSAR, *J. Chem. Inf. Model.* 47 (2007) 2345–2357.
- [63] D.E.V. Pires, T.L. Blundell, D.B. Ascher, pkCSM: Predicting small-molecule pharmacokinetic and toxicity properties using graph-based signatures, *J. Med. Chem* 58 (2015) 4066–4072.
- [64] A. Daina, P. Michielin, V. Zoete, SwissADME: A free web tool to evaluate pharmacokinetics, drug-likeness and medicinal chemistry friendliness of small molecules. *Sci. Rep.* 7 (2017) 42717.
- [65] O. Trott, A.J. Olson, AutoDock Vina: improving the speed and accuracy of docking with a new scoring function, efficient optimization, and multithreading. *J. Comput. Chem.* 3 (2010) 455–461.
- [66] F. Rahim, H. Ullah, M.T. Javid, A. Wadood, M. Taha, M. Ashraf, A. Shaukat, M. Junaid, S. Hussain, W. Rehman, R. Mehmood, M. Sajid, M.N. Khan, K.M. Khan, Synthesis, in vitro evaluation and molecular docking studies of thiazole derivatives as new inhibitors of α -glucosidase, *Bioorg. Chem.* 62 (2015) 15-21.
- [67] Dassault Systèmes BIOVIA. 2016. Discovery studio modeling environment, release 2017, San Diego: Dassault Systèmes. [WWW document], 2016. <http://accelrys.com/products/collaborativescience/biovia-discovery-studio/>. Accessed 25 Feb 17.
- [68] Q. Li, H. Zhang, S. Guan, J. Du, Y. Zhang, S. Wang, Molecular dynamics simulation of the inhibition mechanism of factor XIa by Milvexian-like macrocyclic inhibitors, *Comput. Theor. Chem.* 1225 (2023) 114131.
- [69] M. Ouabane, K. Zaki, M. Alaqarbeh, A. Guendouzi, C. Sekkate, A. Sbai, M. Bouachrine, T. Lakhlifi, Exploring Structure–Toxicity Relationships in Nitrobenzene and Derivatives: A Multifaceted Biochemical Investigation Using 3D–QSPR, HQSPR, Molecular Docking, and MD Simulation, *ChemistrySelect*, 9 (2024) e202304588.

- [70] M.R. Albayati, S. Kansız, N. Dege, S. Kaya, R. Marzouki, H. Lgaz, R. Salghi, I. H. Ali, M.M. Alghamdi, I.M. Chung, Synthesis, crystal structure, Hirshfeld surface analysis and DFT calculations of 2-[(2,3-dimethylphenyl)amino]-N'-[(E)-thiophen-2-ylmethylidene]benzohydrazide, *J. Mol. Struct.* 1205 (2020) 127654.
- [71] Frisch, M. (2009) GAUSSIAN 09. Revision E. 01, Gaussian Inc.
- [72] S. Kaya, C. Kaya, N. Islam, Maximum hardness and minimum polarizability principles through lattice energies of ionic compounds. *Physica B: Condensed Matter*, 485 (2016) 60-66.
- [73] C.A. Lipinski, F. Lombardo, B.W. Dominy, P.J. Feeney, Experimental and computational approaches to estimate solubility and permeability in drug discovery and development settings, *Adv. Drug Deliv. Rev.* 46 (2001) 3-26.
- [74] F.X. Domínguez-Villa, N.A. Durán-Iturbide, J.G. Ávila-Zárraga, J.G. Synthesis, molecular docking, and in silico ADME/Tox profiling studies of new 1-aryl-5-(3-azidopropyl) indol-4-ones: Potential inhibitors of SARS CoV-2 main protease. *Bioorg. Chem.* 106 (2021)104497.
- [75] C.L.D. Ortiz, G.C. Completo, R.C. Nacario, R.B. Nellas, Potential Inhibitors of Galactofuranosyltransferase 2 (GlfT2): Molecular Docking, 3D-QSAR, and In Silico ADMETox Studies. *Sci. Rep.* 9 (2019) 17096.
- [76] B. Kramer, M. Rarey, T. Lengauer, Evaluation of the FLEXX incremental construction algorithm for protein-ligand docking, *Proteins.* 37 (1999) 228–241
- [77] N. Islam, S. Kaya, (Eds.). *Conceptual density functional theory and its application in the chemical domain.* CRC press. (2018).
- [78] R. Çakmak, E. Başaran, S. Kaya, S. Erkan, Synthesis, spectral characterization, chemical reactivity and anticancer behaviors of some novel hydrazone derivatives: Experimental and theoretical insights, *J. Mol. Struct.* 1253 (2022) 132224.
- [79] T. Koopmans, Über die Zuordnung von Wellenfunktionen und Eigenwerten zu den einzelnen Elektronen eines Atoms. *Physica*, 1 (1934) 104-113.
- [80] R.G. Parr, L.V. Szentpály, S. Liu, Electrophilicity index. *J. Amer. Chem. Soc.* 121 (1999) 1922-1924
- [81] S. Kaya, C. Kaya, A new equation for calculation of chemical hardness of groups and molecules. *Mol. Physics.* 113 (2015) 1311-1319.
- [82] S. Kaya, C. Kaya, A new method for calculation of molecular hardness: a theoretical study, *Comput. Theor. Chem.* 1060 (2015) 66-70.
- [83] S. Kaya, D. Ö. Işın, N. Karakuş, Kaya's composite descriptor and Maximum Composite Hardness Rule for chemical reactions. *Journal of the Indian Chemical Society*, 99 (2022) 100364.
- [84] S. Kaya, A. Robles-Navarro, E. Mejía, T. Gómez, C. Cardenas, On the prediction of lattice energy with the Fukui potential: some supports on hardness maximization in inorganic solids. *J. Phys. Chem. A.* 126 (2022) 4507-4516.,
- [85] S. Kaya, C. Kaya, C. A simple method for the calculation of lattice energies of inorganic ionic crystals based on the chemical hardness. *Inorg. Chem.* 54 (20215), 8207-8213.
- [86] E. Chamorro, P.K. Chattaraj, P. Fuentealba, Variation of the electrophilicity index along the reaction path. *J. Phys. Chem. A.* 107 (2003) 7068-7072.

Declaration of interests

The authors declare that they have no known competing financial interests or personal relationships that could have appeared to influence the work reported in this paper.

The authors declare the following financial interests/personal relationships which may be considered as potential competing interests:

Journal Pre-proof